ECMWF Newsletter

Number 147 – Spring 2016

European Centre for Medium-Range Weather Forecasts
Europäisches Zentrum für mittelfristige Wettervorhersage
Centre européen pour les prévisions météorologiques à moyen terme

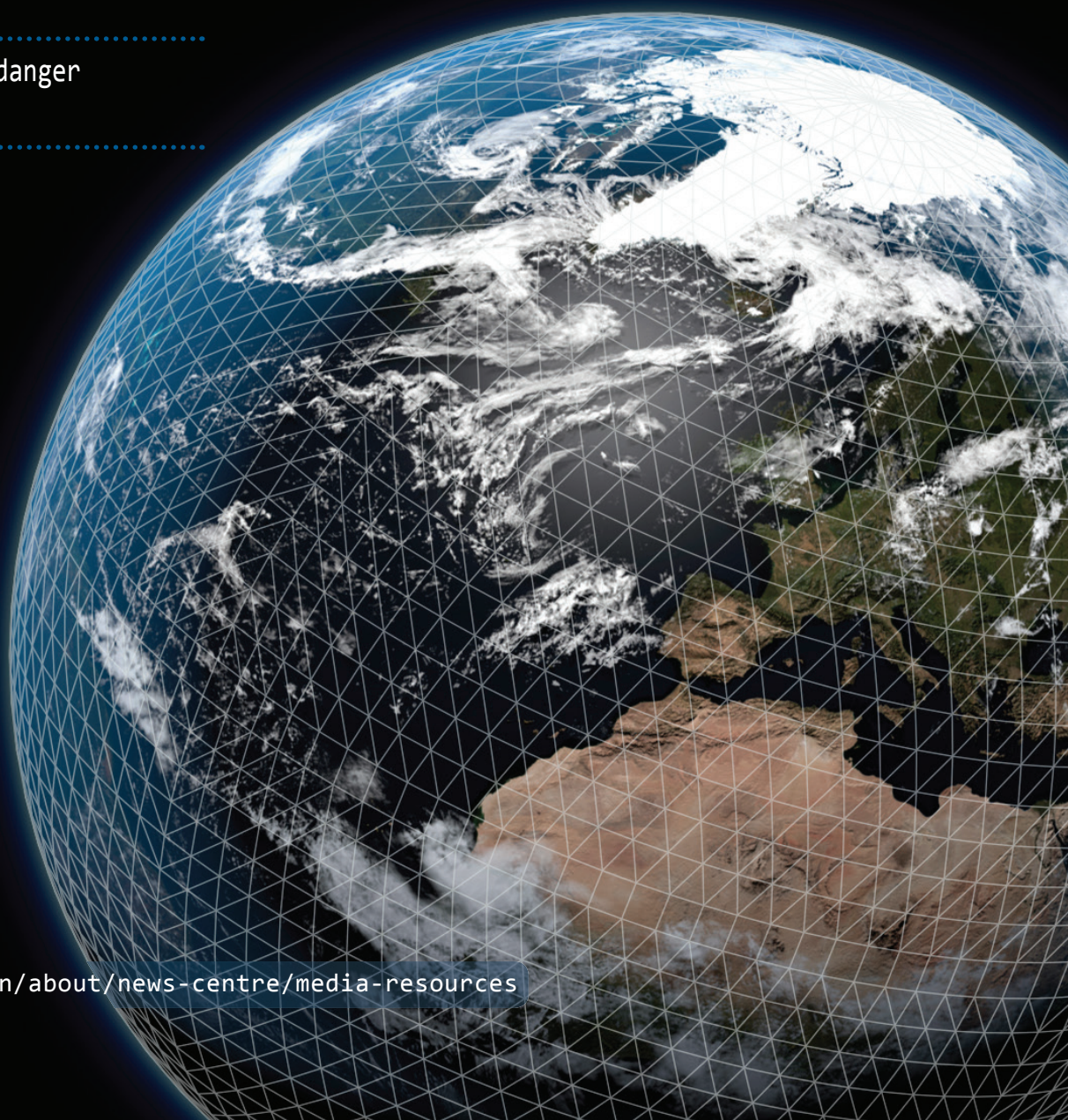

www.ecmwf.int/en/about/news-centre/media-resources

Annual Seminar 2016

Earth system modelling for seamless prediction

On which processes should we focus to further improve atmospheric predictive skill?

5–8 September

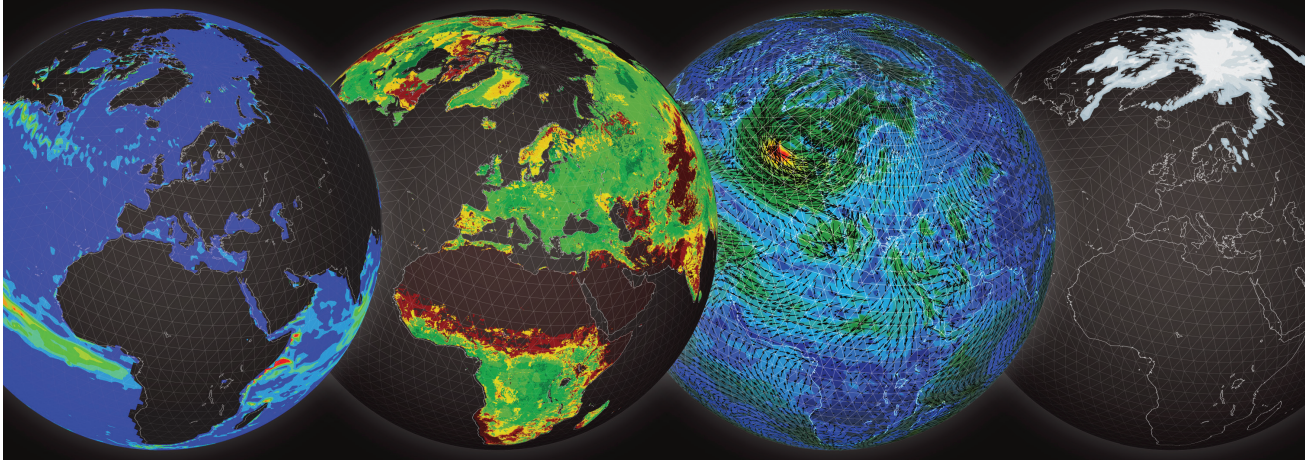

Registration is now open for this year's Annual Seminar. The seminar will explore which Earth system processes need to be represented in global forecasting systems, and what level of complexity is required to further extend atmospheric predictive skill. Key questions that will be addressed are: If we want to improve the skill of weather predictions, on which of the already-simulated processes should we focus? If we introduce new processes, how much complexity is actually required?

The 22 invited speakers come from ECMWF and from meteorological services, universities and research centres across the world. They will present progress and challenges in different areas of Earth system modelling. Speakers will also address implementation aspects, including system design and coupling strategies in forecasting and initialisation as well as in reanalyses.

ECMWF

email: **events@ecmwf.int**

http://www.ecmwf.int/en/learning/workshops-and-seminars/en/annual-seminar-2016

CONTENTS

PUBLICATION POLICY

The *ECMWF Newsletter* is published quarterly. Its purpose is to make users of ECMWF products, collaborators with ECMWF and the wider meteorological community aware of new developments at ECMWF and the use that can be made of ECMWF products. Most articles are prepared by staff at ECMWF, but articles are also welcome from people working elsewhere, especially those from Member States and Co-operating States. The *ECMWF Newsletter* is not peer-reviewed.

Editor: Georg Lentze

Typesetting and Graphics: Anabel Bowen with the assistance of Simon Witter.

Cover illustration based on an image from: mrgao/iStock/Thinkstock

Any queries about the content or distribution of the *ECMWF Newsletter* should be sent to Georg.Lentze@ecmwf.int

Guidance about submitting an article is available at www.ecmwf.int/en/about/news-centre/media-resources

CONTACTING ECMWF

Shinfield Park, Reading, Berkshire RG2 9AX, UK

Fax:		+44 118 986 9450
Telephone:	National	0118 949 9000
	International	+44 118 949 9000
ECMWF website:		www.ecmwf.int

Progress

The previous edition of the Newsletter provided an insight into the years of research that went into the development and implementation of one of the most substantial model upgrades our Integrated Forecasting System (IFS) has undergone in many years. IFS Cycle 41r2 is set to offer improved range, reliability and accuracy to help national meteorological services provide earlier warnings of adverse conditions and extreme weather to better protect property and vital infrastructure, and to aid long-term planning for weather-dependent industries.

Several weeks into the new model cycle becoming operational, we can report a smooth transition with extremely limited disruption to users, which in itself is an achievement. Most importantly, the evaluation results presented in this Newsletter give us great confidence in the quality of 41r2 analyses and forecasts. How did we get here?

The first ingredient is of course the research that ECMWF conducts into all aspects of numerical weather prediction (NWP), from the modelling of physical processes to the development of new numerical schemes and data assimilation methods. The second ingredient is the exchange of ideas and solutions with our Member State partners and through academic collaborations, for example the recent adaptation of the input/output server. Last but certainly not least, the upgrading and expansion of our supercomputers from Cray XC30s to Cray XC40s will deliver the computing capability needed to make it all work.

The model upgrade illustrates how intimately linked progress in NWP is with supercomputing and the scalability of NWP codes. This is why we were delighted to be invited to host the Cray User Group meeting 2016 in London, which is dedicated to the overarching theme of scalability. This gathering of some 200 supercomputing experts is held once a year to review and discuss developments at Cray, and sometimes to challenge the American vendor. But the conference, which takes place from 8 to 12 May, is also about ensuring that Cray and its users have a platform for sharing ideas and prospects for development.

Our Scalability Programme is taking the same approach, teaming up forecasting experts with university research and high-performance computing centres as well as world-leading hardware companies to bring entirely new knowledge and technology to the field. The close partnership we have enjoyed with computing vendors over the years has played a critical role in ensuring ECMWF's success and is one of our key priorities, as our Workshop on High-Performance Computing in Meteorology to be held in November will once again illustrate this year.

Maintaining a strong and constant dialogue with the computing industry has proven to be in all our best interests. It ensures that advances in computing match what our science requires – which is a win for them and for us – and it also ensures that we can take research in NWP to the frontiers of knowledge, producing the best possible predictions for the benefit of our Member and Co-operating States.

Florence Rabier
Director-General

Wind and wave forecasts during Storm Gertrude/Tor

LINUS MAGNUSSON,
JEAN BIDLOT

ECMWF forecasts provided early indications of a windstorm that hit north-western Europe at the end of January 2016. Predicted winds and waves were slightly lower than those observed at North Sea oil platforms, but ensemble wave forecasts produced using ECMWF's new higher-resolution model matched observations reasonably well.

The winter 2015–2016 started with a positive phase of the North Atlantic Oscillation (NAO), resulting in warm, windy and rainy weather in north-western Europe during December. The central and northern parts of the British Isles experienced two episodes of severe flooding after storms Desmond and Eva. In January, the weather turned colder in northern Europe with a weaker westerly flow. However, the positive NAO phase returned in the last days of January, bringing a severe windstorm to this part of Europe.

The cyclone, named Gertrude in the UK and Tor in Norway, formed south of Iceland late on 28 January. It rapidly deepened by 30 hPa during the next 24 hours and reached 948 hPa late on 29 January. Red warnings for extreme winds and high waves were issued for Shetland and the southern half of Norway, and amber warnings for Scotland. In Scotland, wind gusts of up to 50 m/s were measured. When the storm made landfall on the Norwegian coast, a new record mean wind speed for Norway was measured at Kråkenes fyr (lighthouse): a 10-minute average of 48.9 m/s, with gusts of up to 62 m/s. Fortunately, the storm did not cause any fatalities, and only limited damage was reported. This can partly be attributed to early warnings. ECMWF forecasts gave a clear indication of extreme winds six days in advance.

The band of the strongest winds stretched from Shetland towards the western part of Norway and passed the oil fields in the North Sea. Many of the oil platforms submit meteorological and wave observations every hour. This provided an opportunity for a detailed evaluation of ECMWF's wave forecasts produced by the new model cycle 41r2 under extreme conditions, with significant wave heights up to 14 metres. With hourly data from the model, we can compare both the model cycle operational at the time (41r1) and the new model cycle (implemented on 8 March 2016) with observations from an oil platform located at 61.2°N, 1.1°E.

All of the last three forecasts before the peak of the event (28 Jan 12 UTC, 29 Jan 00 UTC and 12 UTC) underestimated the intensity of the peak in the mean wind at the oil platform (28 m/s compared to 38 m/s in the most extreme observation – not shown). However, one has to bear in mind that the measurements are probably made at a height greater than 10 metres and would have to be calibrated for a proper comparison with 10-metre wind forecasts produced by the model. For the wind speed, both model versions give similar values. The maximum significant wave height is also somewhat underestimated (12 metres in the forecast from 29 Jan 00 UTC compared to 14 metres in observations). Comparing the forecasts

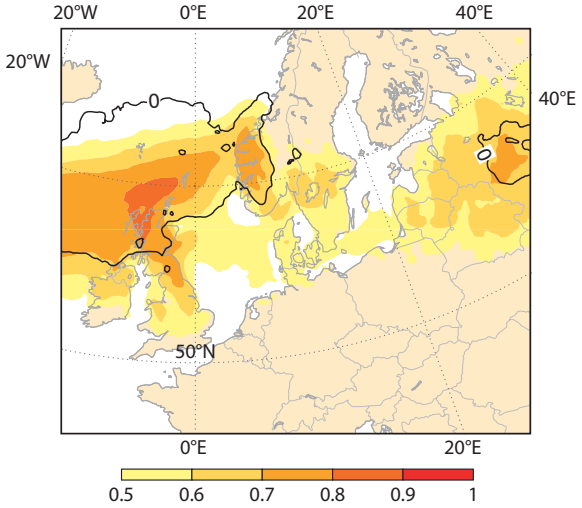

Extreme Forecast Index (EFI) and Shift of Tails (SOT). The chart shows the EFI (shading) and SOT (contours) for 10-metre wind gusts for the forecast from 00 UTC 24 January valid on 29 January (00-24 UTC).

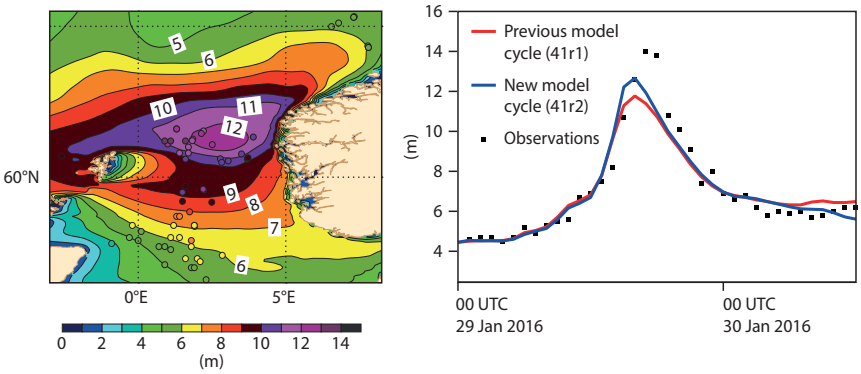

High-resolution wave forecasts and observations. The left-hand panel shows ECMWF's 18-hour high-resolution significant wave height forecast from 00 UTC on 29 January (shading) produced using the new model cycle 41r2, and raw observations (circles). The right-hand panel shows observations from an oil platform located at 61.2°N, 1.1°E, and high-resolution forecasts (HRES) for the nearest grid point from 00 UTC on 29 January produced using the previous model cycle 41r1 and the new model cycle 41r2.

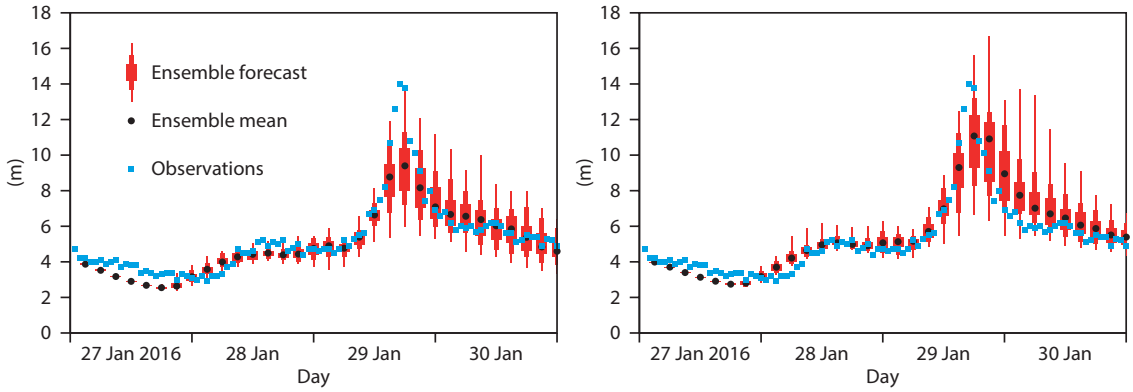

Ensemble wave forecasts and observations. Ensemble forecasts of significant wave height from 00 UTC on 27 January 2016 for 61.2°N, 1.1°E, from the previous model cycle 41r1 (left) and the new model cycle 41r2 (right), and observations.

from the two model cycles, the wave forecast produced by the new model was about 1 metre higher at the peak of the event despite predicting similar wind speeds. This is due to the increased horizontal resolution both in the atmospheric model (9 km grid spacing instead of 16 km) and in the wave model (14 km instead of 28 km), as previously demonstrated for a severe storm that hit the Faroe Islands in November 2011.

The ensemble forecast from the new model shows more extreme scenarios than that produced by the old model, and observed waves are within the range of uncertainty indicated by the forecast from 27 January 00 UTC. For this part of the North Sea, ensemble forecasts are essential as a small difference in the cyclone path can make a large difference in wave fields because of the sheltering effect of the Shetland Islands.

Forecasts aid mission planning for hurricane research

SHARAN MAJUMDAR
(University of Miami, USA),
ALAN BRAMMER
(University at Albany, USA)

ECMWF forecasts have helped researchers in the United States to plan the deployment of aircraft in a field experiment on tropical cyclone intensity and structure change. The 2015 Tropical Cyclone Intensity field experiment (TCI-15), funded by the US Office of Naval Research, sampled the upper-level outflow of tropical cyclones in order to reveal new insights into the role that outflow might play in intensity change.

The field experiment involved the deployment of the NASA WB-57 aircraft, which possessed a unique capability to fly over the cyclones and deploy up to 80 dropwindsondes per mission. Two noteworthy cases were Hurricane Joaquin in the Atlantic basin, which possessed unusually high uncertainty in its forecast, and Hurricane Patricia in the eastern Pacific basin, which was the most intense tropical cyclone ever recorded in the western hemisphere.

Hurricane Joaquin

On 27 September 2015, the TCI team's focus had been on Hurricane Marty near Mexico. However, the 00 UTC ECMWF ensemble began to suggest that a loosely organised cluster of thunderstorms north of the Dominican Republic had the potential to develop into a tropical cyclone. This indication helped convince the TCI team to forward deploy the aircraft, crew and equipment to Georgia in the eastern United States, in order to prepare for missions over the disturbance that ultimately became Hurricane Joaquin.

The consistency in ECMWF's high-resolution and ensemble output over this period led to increased confidence that this would be an excellent case. Four WB-57 missions over Joaquin were conducted between 2 and 5 October, including the period when Joaquin was a Category 4 hurricane.

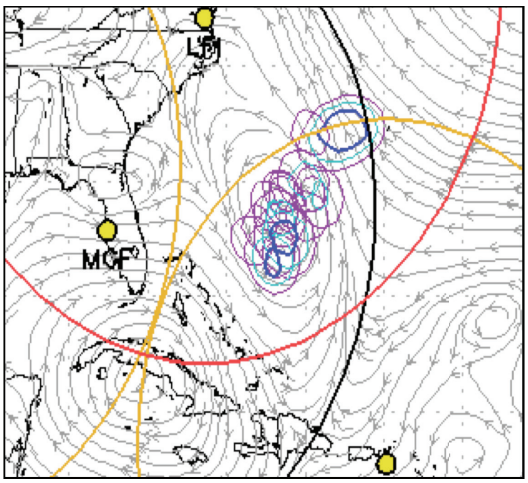

Ensemble forecast of relative vorticity linked to Hurricane Joaquin. This three-day ECMWF ensemble forecast from 00 UTC on 27 September 2015 showed a range of scenarios for relative vorticity averaged over 700–850 hPa: magenta contours correspond to a vortex whose strength is commensurate with a tropical cyclone, while blue contours indicate stronger vortices. The ensemble forecast gave an early indication of Joaquin's development. Large circles (black, yellow, red) indicate the potential range of WB-57 aircraft from various bases.

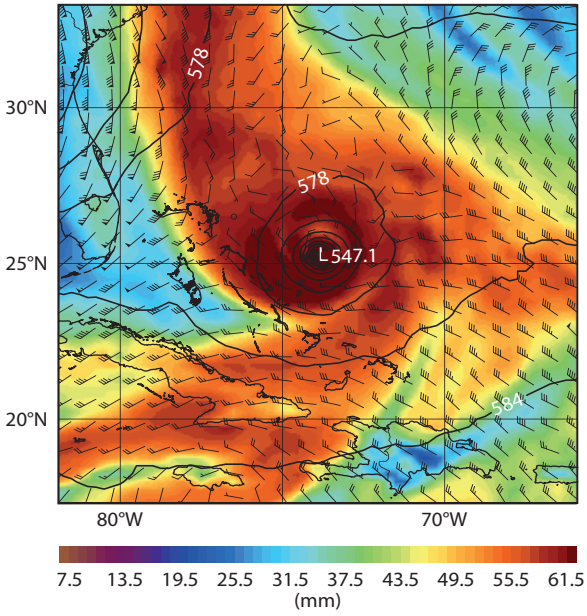

High-resolution forecast of Hurricane Joaquin. ECMWF's 4-day high-resolution forecast of total precipitable water (shading), 200 hPa wind (barbs) and 500 hPa height (contours, in decametres) from 00 UTC on 29 September 2015 suggested an intense Hurricane Joaquin with outflow towards the north and east.

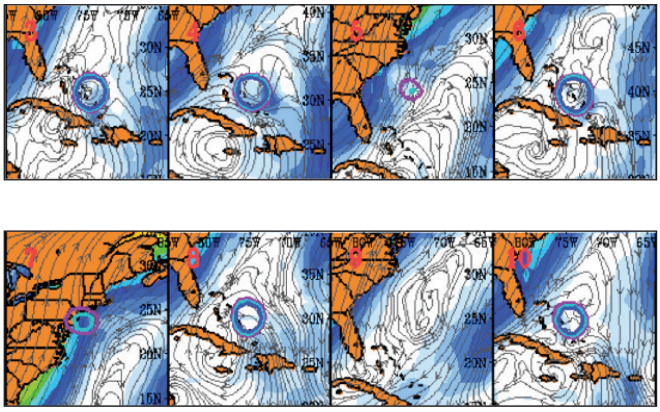

Ensemble 'postage stamps' of Hurricane Joaquin. Different members of this three-day high-resolution and ensemble forecast for Joaquin from 00 UTC on 29 September 2015 indicated different scenarios for the strength of the hurricane vortex and outflow configurations.

ECMWF's high-resolution forecasts were the earliest of all forecasts from operational models to capture the correct track of the hurricane.

Beyond the decision of whether or not to deploy, additional decisions on how to design the flight tracks were also necessary. To address the scientific goal of understanding the role of the upper-tropospheric outflow in tropical cyclone intensity change, new products based on ensemble forecasts were developed and used. These products demonstrated the range of scenarios, not only of the position and strength of the hurricane, but also of the configuration of the outflow.

Hurricane Patricia

ECMWF's high-resolution and ensemble forecasts were also used to guide the planning of the historic missions into Hurricane Patricia, which possessed a minimum sea-level pressure of 872 hPa and a maximum sustained wind speed of 95 m/s on 23 September 2015. The time-sensitive decision on deployment, which resulted in four successful WB-57 missions, can again be attributed in large part to the quality of the forecast guidance.

Conclusion

The TCI-15 field experiment benefited substantially from ECMWF's forecasts, which were the central predictions used during the daily weather briefings. Especially due to the complicated logistics of forward deployment, which needed to be initiated several days prior to the missions, accurate estimations of the likelihood of a significant tropical cyclone for sampling were necessary. The retrospective consensus view of the TCI-15 team is that all the decisions on deployment (or non-deployment) turned out to be the correct call, which speaks to the effectiveness of the model guidance.

The TCI team are grateful for the excellent support provided by the ECMWF Data Services team, and the reliable timely transfer of the data. Now that the field experiment has concluded, investigators are using the data to address scientific questions related to the dynamics and predictability of tropical cyclones.

Hurricane Patricia from above. Looking down on Hurricane Patricia from aboard the WB-57 aircraft. (*Photo: Joe Gerky*)

ECMWF helps to probe impact of aerosols in West Africa

ANGELA BENEDETTI, FRÉDÉRIC VITART (both ECMWF), **PETER KNIPPERTZ** (Karlsruhe Institute of Technology, Germany)

Southern West Africa (SWA) is becoming a focus of interest for climate change and air quality studies due to its rapid population growth and economic expansion. Much of this population will be concentrated in urban centres, and atmospheric emissions of chemical compounds and aerosols from industrial, transport, and energy sectors in the area are likely to increase. These changes are expected to affect human health, ecosystems and biodiversity, and regional climate.

ECMWF is a partner in the DACCIWA (Dynamics–Aerosol–Chemistry–Cloud Interactions in West Africa) project, which aims to provide a comprehensive assessment of these impacts and to provide scientific support for the region's sustainable development. This EU-funded project runs from 1 December 2013 until 30 November 2018. It involves 16 partners (universities, research institutes, and operational weather and climate centres) from European and West African countries and is co-ordinated by the Karlsruhe Institute of Technology (KIT). DACCIWA builds on a number of past and existing projects and networks in West Africa, including the African Monsoon Multidisciplinary Analysis (AMMA).

Field campaign

A lack of observations is a major obstacle to achieving DACCIWA's objectives. To alleviate this, DACCIWA will carry out a major field campaign in SWA during June and July 2016, involving co-ordinated flights with three research aircraft and a wide range of surface-based instrumentation at Kumasi, Ghana; Savé, Benin; and Ile-Ife, Nigeria. June–July marks the onset of the West African Monsoon. The increased cloudiness this brings is susceptible to aerosol effects and important for radiation.

ECMWF has an interest in studying West Africa since model errors are particularly evident in the tropics and have implications for predictability in the mid-latitudes. ECMWF actively participated in AMMA by assessing how additional observations can improve analyses and forecasts in the region. It was found that extra soundings had a significant impact on the ECMWF analysis, particularly for low-level temperature over the Sahel and the structure of the African easterly jet. However, the impact on forecasts disappeared after 24 hours. Large model biases in boundary layer temperature over the northern and eastern Sahel were found, consistent with well-known model biases in cloud, rainfall and radiation.

Impact of aerosols

ECMWF's contribution to DACCIWA will include providing forecasts for the June–July field campaign in collaboration with the Copernicus Atmosphere Monitoring Service (CAMS) campaign support team (Luke Jones and Miha Razinger). ECMWF will also design and run ad hoc experiments for West Africa. These will include medium-range runs with interactive aerosols using the Composition-Integrated Forecasting System (C-IFS) and seasonal runs based on the operational monthly ensemble forecasts. The experiments will serve to assess the importance of aerosols for the West African Monsoon onset and development. Work towards this goal has already started and has led to a multi-year run (2003–2015) with interactive aerosols, which is currently being compared with the operational monthly system. Preliminary results

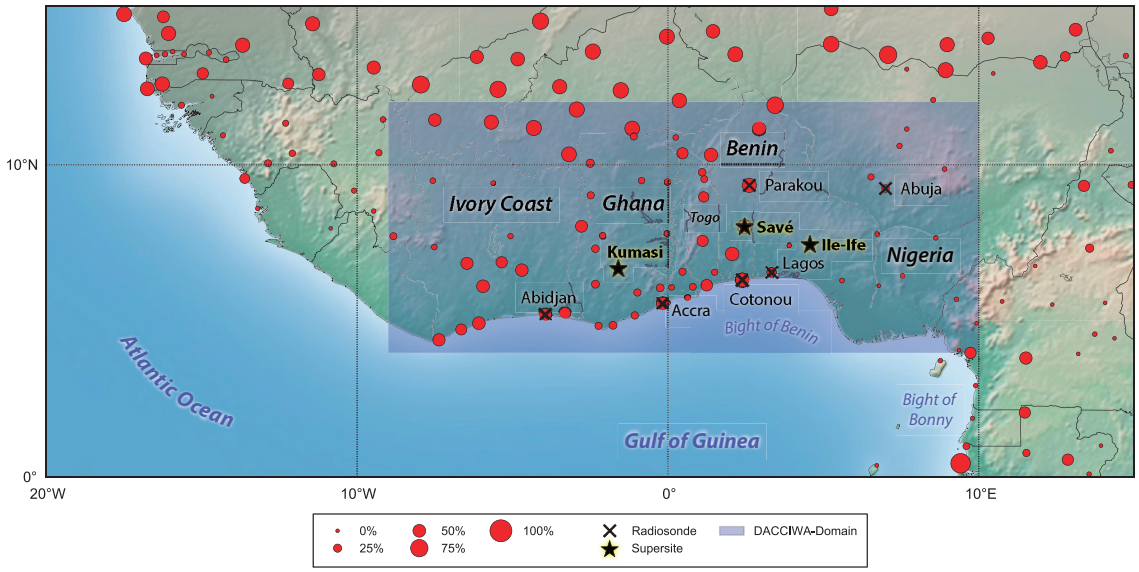

DACCIWA field campaign. Black stars mark the three DACCIWA supersites at Kumasi, Ghana; Savé, Benin; and Ile-Ife, Nigeria. Red dots mark synoptic weather stations. The size of the dots is proportional to the available number of reports in the WMO Global Telecommunication System from 1998 to 2012. (*Source: P. Knippertz et al., Bull. Am. Meteorol. Soc., September 2015, 1451–1460*)

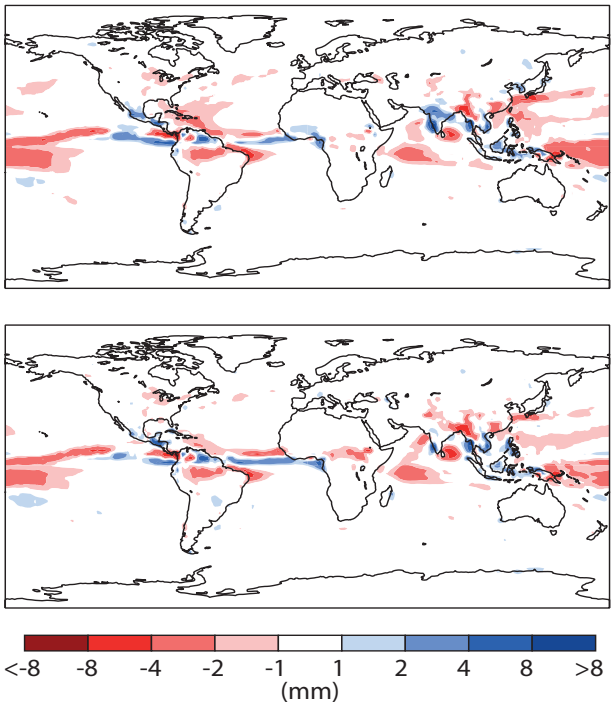

show that including aerosols in the model has a positive impact on weather predictions by reducing the wet bias in precipitation over land in SWA. Forecasts for other areas, such as India and the West Atlantic, also appear to improve in the interactive aerosol run. More cases are needed to assess the impact of including aerosols on the skill of the monthly forecast and to fully evaluate aerosol fields over seasonal scales.

For more details on DACCIWA, visit www.dacciwa.eu.

Reduced rainfall bias. The charts show the bias in rainfall forecasts for the month of June in the control run (top) and the interactive aerosol run (bottom). The bias is calculated over the period 2003-2015 with respect to the ERA-Interim climate reanalysis.

Croatian flag to be raised at the Centre on 30 June

JOANNE JEPPESEN

The Croatian flag will be raised at the Centre's headquarters in Reading on 30 June after Croatia became ECMWF's 22nd Member State on 1 January 2016. The ceremony will take place in the presence of representatives from all ECMWF Member States gathered for the Centre's summer Council meeting.

Accession to full membership marks the next step for co-operation between ECMWF and Croatia. As a Member State, Croatia now has access to a share of the Centre's supercomputing and archive resources for its own use, as well as voting rights at the ECMWF Council. It continues to have full access to ECMWF's products and services as it did under the co-operation agreement it concluded with the Centre in December 1995.

Mr Ivan Čačić, the Director of the Croatian Meteorological and Hydrological Service (DHMZ) and Croatia's Permanent Representative to the WMO, said he was delighted that Croatia had established this formal link with ECMWF. He stressed that Croatia would work to "support the potential and position of ECMWF as an organisation and also as a crucial entity of the European Meteorological Infrastructure".

ECMWF Director-General Florence Rabier said that, after some 20 years of working closely with Croatia as a Co-operating State and as a member of the ALADIN consortium, it was "excellent news that Croatia will now have an opportunity to be part of our Council, hence helping to set the Centre's strategic direction for the years to come".

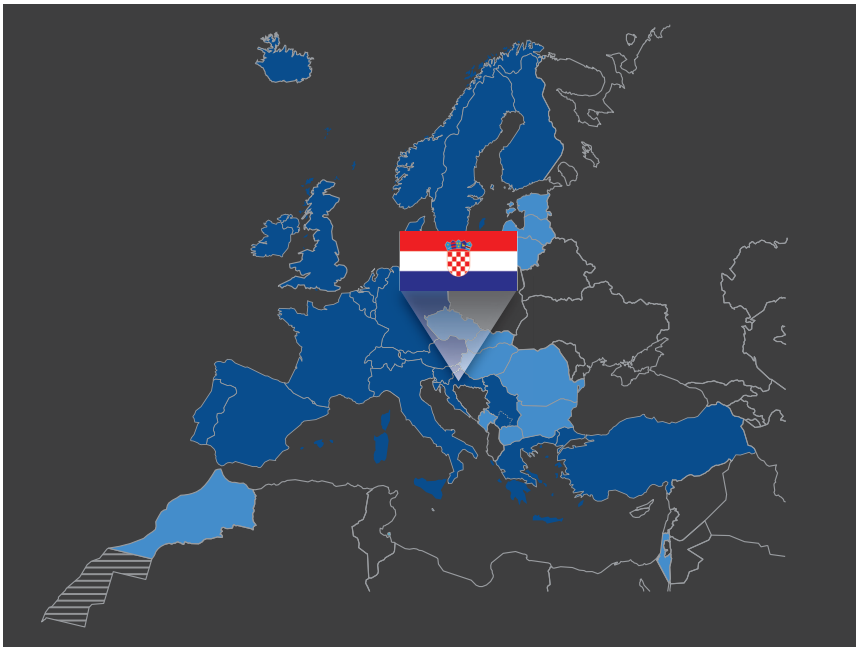

ECMWF's Member and Co-operating States. Croatia officially became a Member State on 1 January 2016. ECMWF now has 22 Member States (dark blue) and 12 Co-operating States (light blue).

ERA5 reanalysis is in production

HANS HERSBACH, DICK DEE

After many years of research and a great deal of technical preparation, the production of a new ECMWF climate reanalysis to replace ERA-Interim has started. ERA5 will be the fifth generation of ECMWF atmospheric reanalyses of the global climate, which started with the FGGE reanalyses produced in the 1980s, followed by ERA-15, ERA-40 and most recently ERA-Interim.

Reanalyses provide a numerical description of the recent climate by combining models with observations. They have been invaluable to numerous users in Member States and around the world and have always been closely associated with the excellence of the Centre's forecast products. Reanalysis is now a key ECMWF contribution to the implementation of the EU-funded Copernicus Climate Change Service. This is reflected by the fact that ERA5 is the first reanalysis produced as an operational service rather than a research project.

Once complete, approximately two years from now, the new ERA5 reanalysis will span the modern observing period from 1979 onward, with daily updates continuing forward in time. ERA5 will eventually replace ERA-Interim, which is increasingly difficult to maintain. ERA5 data will be at a much higher resolution than ERA-Interim: hourly analysis fields will be available at a horizontal resolution of 31 km on 139 levels, from the surface up to 0.01 hPa (around 80 km).

All ERA5 data products will include information about uncertainties, which will be provided for each parameter at 3-hourly intervals and at a horizontal resolution of 62 km. Many new parameters, such as 100-metre wind speed and direction, will be available as part of the output. A database containing all ingested observations, together with detailed information about how they are used, will be available and accessible to users. Altogether, the entire ERA5 production will generate roughly 5 petabytes of data.

The research conducted at ECMWF since the start of ERA-Interim in late 2006 gives us great confidence in the quality of the ERA5 reanalysis. The ERA5 data assimilation system uses the current version of the Integrated Forecasting System (IFS Cycle 41r2), with several added features specifically developed for reanalysis. The many changes and improvements incorporated into the IFS represent a decade of research and development in modelling and data assimilation. The ERA5 reanalysis will also benefit from the research conducted in the EU-funded ERA-CLIM and ERA-CLIM2 projects carried out by ECMWF and partners. These have led to improved input data for the assimilating model that better reflect observed changes in climate forcings, as well as many new or reprocessed observations for data assimilation.

Some of the main characteristics and innovations in ERA5 with respect to ERA-Interim are listed in the table.

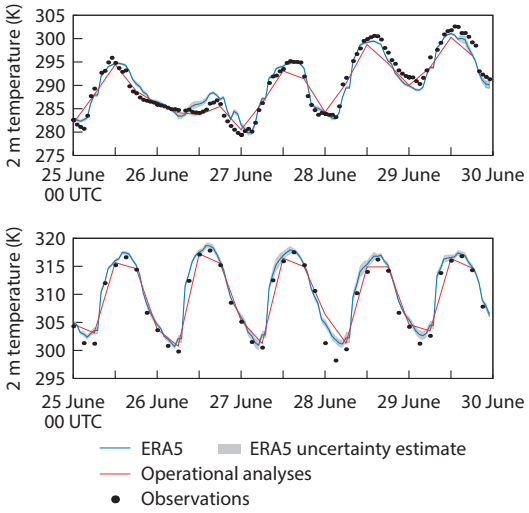

ECMWF operational analyses and ERA5 reanalysis. The charts show hourly data from 25 to 30 June 2014 from ECMWF's operational analyses and the ERA5 reanalysis of 2-metre temperature compared to in-situ observations at the Instytut Meteorologii i Gospodarki Wodne near Krakow in Poland (coordinates: 50.03°N, 20.25°E) (top) and a location in the Sahara Desert (coordinates: 26.5°N, 8.42°E) (bottom).

	ERA-Interim	ERA5
Period	1979 – present	1979 – present
Production period	August 2006 – end 2018	Jan 2016 – end 2017, then continued in near real-time
Assimilation system	IFS Cycle 31r2	IFS Cycle 41r2
Model input	As in operations (inconsistent SST)	Appropriate for climate (e.g. CMIP5 greenhouse gases, volcanic eruptions, SST and sea-ice cover)
Spatial resolution	79 km globally, 60 levels to 0.1 hPa	31 km globally, 137 levels to 0.01 hPa
Uncertainty estimates	None	From a 10-member Ensemble of Data Assimilations (EDA) at 63 km resolution
Output frequency	6-hourly analysis, 3-hourly forecast fields	Hourly analysis and forecast fields, 3-hourly for the EDA
Input observations	As in ERA-40 and from Global Telecommunication System	In addition, various newly reprocessed datasets and recent instruments that could not be ingested in ERA-Interim
Variational bias scheme	Satellite radiances	Also ozone, aircraft and surface pressure data
Satellite data	RTTOV-7, clear-sky	RTTOV-11, all-sky for various components
Additional innovations		Long-term evolution of CO_2 in RTTOV, cell-pressure correction SSU, improved bias correction for radiosondes, EDA perturbations for sea-ice cover

Supercomputer upgrade is under way

MIKE HAWKINS

On 19 February 2016, the Centre received the first pieces of equipment supplied as part of a significant upgrade of its supercomputers. The additional Cray Sonexion 2000 storage was delivered under a 36-million-dollar contract signed earlier this year with Cray Inc. The deal will see the current Cray XC30 supercomputers upgraded and expanded to Cray XC40 systems.

The upgrade involves adding a new cabinet to each supercomputer, taking it from 19 cabinets to 20, and swapping all the existing compute blades in each machine for new ones with the latest generation of Intel Xeon processors.

Another step in the upgrade took place at the end of March, when there was a short outage to install new nodes. A seven-week user test period is now under way, during which 25,000 cores will be available on one cluster for people to test codes at scale. This testing step is extremely important: we need to be sure that we can run our forecast codes on the upgraded machines and be sure of the results before we commit to the next stage in the process.

First delivery. The four racks of Cray Sonexion storage delivered in February will provide an extra five petabytes of storage, enough space to store a billion copies of the complete works of Shakespeare.

In the next step, Cray will take each supercomputer out of service for a week to swap approximately 900 blades in each machine. When the upgrade is complete, the result will be two identical machines, each with more than 130,000 cores of the latest Intel Xeon 'Broadwell' processor – 55% more than a current cluster – and more than double the amount of memory. Cray will also supply a 32-node Cray XC40-AC system with the next generation of the Intel Xeon Phi processor.

"*This upgrade will help us to improve the quality of the service we provide to our Member and Co-operating States*," ECMWF Director of Research Erland Källén said. "*It will enable us to develop high-resolution ensemble forecasts that improve the prediction of severe weather events in the medium range, up to about two weeks ahead. It will also make it possible to introduce improved data assimilation methods, allowing us to use more of the available Earth system observations, and to produce more detailed and better-quality atmospheric composition forecasts as well as high-quality climate datasets (reanalyses).*"

ECMWF steps up work on I/O issues in supercomputing

ANTONINO BONANNI,
TIAGO QUINTINO,
SIMON SMART

ECMWF presented its plans for an input/output (I/O) Workload Simulator during an international meeting at the Centre on 23 and 24 February. The event brought together the eight partner organisations involved in the NEXTGenIO project on I/O challenges in supercomputing.

NEXTGenIO aims to develop innovative solutions to tackle input/output (I/O) bottlenecks as high-performance computing (HPC) moves towards exascale capabilities. The project started on 1 October 2015 and is set to run for three years. It is a Horizon 2020 EU-funded project with an 8.1m-euro budget and is co-ordinated by the Edinburgh Supercomputing Centre (EPCC). The outcome of the project will be a prototype HPC system designed by Fujitsu with Intel 3D-XPoint Non-Volatile RAM (NVRAM), including newly developed systemware and an adapted application stack.

Workload Simulator

As one of the main application providers, ECMWF is contributing by developing an I/O Workload Simulator (IOWS), which will be used to evaluate the new HPC system and may be used in future HPC procurement.

The IOWS aims to simulate workloads from real HPC systems, both theoretically by means of software and practically by using a collection of lightweight, portable applications on real hardware. To do this, it will record metrics on operational systems. The recorded workload will be interpreted and modelled to reduce its complexity and gain insights into its structure. This model will then be simulated in software, which will permit an analysis of how varying the properties of the workload or of the hardware impacts the overall workflow.

The IOWS will also be able to execute the modelled workload on a physical HPC system, and it will ideally permit

the scaling of modelled workloads for deployment on prototype HPC systems during development or procurement.

I/O libraries in the IFS

ECMWF will also adapt the I/O libraries in the Integrated Forecasting System (IFS) to take advantage of NVRAM technology and reduce the impact of I/O on daily operations. Currently, data is written to a parallel disk-based storage system between each of the components of the operational system (for example between the IFS and Product Generation). This forms a growing bottleneck as the volume of data generated increases. As part of the project, NVRAM will be used as a large, distributed, caching layer to connect different components of the operational system. This will minimise the usage of disk-based I/O in the time-critical path.

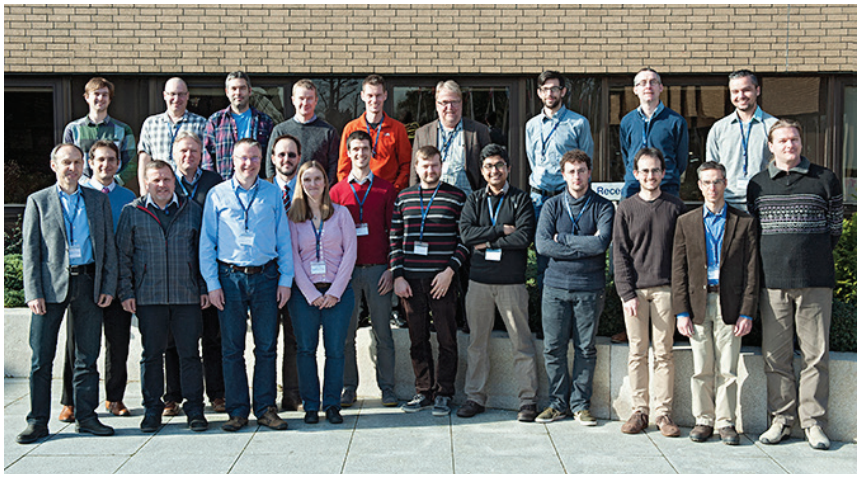

Participants in the NextGenIO meeting. NextGenIO project members met at ECMWF in February 2016.

The Copernicus Climate Change Service Sectoral Information Systems

JEAN-NOËL THÉPAUT

As part of the implementation of the EU-funded Copernicus Climate Change Service (C3S), ECMWF aims to develop Sectoral Information Systems (SIS), which will provide sector-specific shop windows for the C3S Climate Data Store. Several SIS proof-of-concept projects are now under way. They will serve to develop tools and products which will be tested directly with users from sectors to which climate information is particularly relevant.

From these proof-of-concept projects, and based on interactions with users, C3S will select a set of tailored sectoral climate indicators to be routinely produced and visualised. It will support the tools and promote best practices so that these sectors can take advantage of C3S climate information to enhance their businesses.

There are seven proof-of-concept projects, focusing on water (2); energy (2); insurance; agriculture; and infrastructure & health.

Each proof-of-concept is run by a consortium of organisations that bring sector-specific expertise to the projects. The primary partners working with ECMWF under the auspices of the European Union's Copernicus Earth observation programme are:

- The Swedish Meteorological and Hydrological Institute (SMHI) for the Service for Water Indicators in Climate Change Adaption (SWICCA) project (Water) and the UrbanSIS project (Infrastructure & Health)
- The University of East Anglia for the European Climatic Energy Mixes (ECEM) project (Energy)
- Telespazio for the Agriclass project (Agriculture)
- CGI for the Wind Storm Climate Service (WISC) project (Insurance)
- The Centre for Ecology and Hydrology (CEH) for the End-to-end Demonstrator for Improved Decision Making in the Water Sector in Europe (EDgE) project (Water)
- Le Laboratoire des Sciences du Climat et de l'Environnement (LSCE) for the Clim4energy project (Energy).

Spotlight on water

Water and climate change are inextricably linked. Increases in temperature, shifts in precipitation patterns and snow cover and a likely increase in the frequency of flooding and droughts all pose challenges for the water management sector. C3S aims to help the water industry and policymakers tackle these challenges. Changes in Europe's water resources will also have consequences for several other sectors, particularly agriculture, forestry, energy and health.

In recognition of this, two water–related contracts have been concluded as part of the SIS work.

- The Service for Water Indicators in

Copernicus at ECMWF

C3S is being implemented by ECMWF on behalf of the European Commission. It is part of the EU's flagship Copernicus Earth observation programme, which delivers freely accessible environmental information services. ECMWF has also been entrusted with operating the Copernicus Atmosphere Monitoring Service (CAMS), which provides daily forecasts of atmospheric composition from the ground up to the stratosphere, and it contributes to the Copernicus Emergency Management Service (Copernicus EMS), which provides information relevant to the management of natural disasters, human-made emergency situations, and humanitarian crises.

Copernicus
Europe's eyes on Earth

Climate Change Adaption (SWICCA)

- The End-to-end Demonstrator for Improved Decision Making in the Water Sector in Europe (EDgE)

SWICCA

The SWICCA proof-of-concept project aims to:

- Advance the functionality and content of C3S to meet the needs of the water management sector
- Provide pan-European climate impact indicators based on the most relevant variables and indices for water management across Europe
- Gather a European community of consultants or 'purveyors' to the water sector to ensure that there is uptake of C3S through appropriate design and useful content.

SWICCA puts a strong emphasis on consultants or 'purveyors'. These people are a crucial part of the SWICCA 'ecosystem', advising water managers and policymakers on all areas of water-related business and decision-making. They have the tools to translate, transform and visualise data and merge it with local information to create practical products for their clients. SWICCA will reach out to these intermediaries and form a community that will guide the development, design and use of the proof-of-concept project.

EDgE

EDgE will bring together a group of water management practitioners, hydrological experts and environmental information analysts qualified to define and develop climate impact indicators that will be of operational value to the water sector in Europe.

Using modelling – for both climate and hydrological impact – EDgE will produce terrestrial Essential Climate Variables (tECVs) specific to the water sector for past, current and future time horizons. In so doing it will contribute to the efforts of Climate-ADAPT and the WMO Global Framework for Climate Services (GFCS), among others.

EDgE will also deliver new Sectoral Climate Impact Indicators (SCIIs) co-designed with users from the European water sector community. The project will involve users in the UK, Norway and Spain, bringing them together in phases:

- Phase 1: Design, to establish current users' requirements, decision contexts and practices, and to provide an assessment of candidate SCIIs and the SIS prototype and recommend specification for new products and SIS services
- Phase 2: Testing, to assess the proposed SCIIs and stage 2 Demonstrator prototype, and to refine the Demonstrator functionalities and make recommendations on language and accessibility
- Phase 3: Implementation, to review the final Demonstrator prototype and user guidance and to make final recommendations.

The project team itself includes representatives from regulatory institutions at European and national levels, government departments and policymakers, regional and local authorities, science and industry.

More information on the C3S Sectoral Information System proof-of-concept projects is available on the C3S website: http://climate.copernicus.eu/resources/information-service

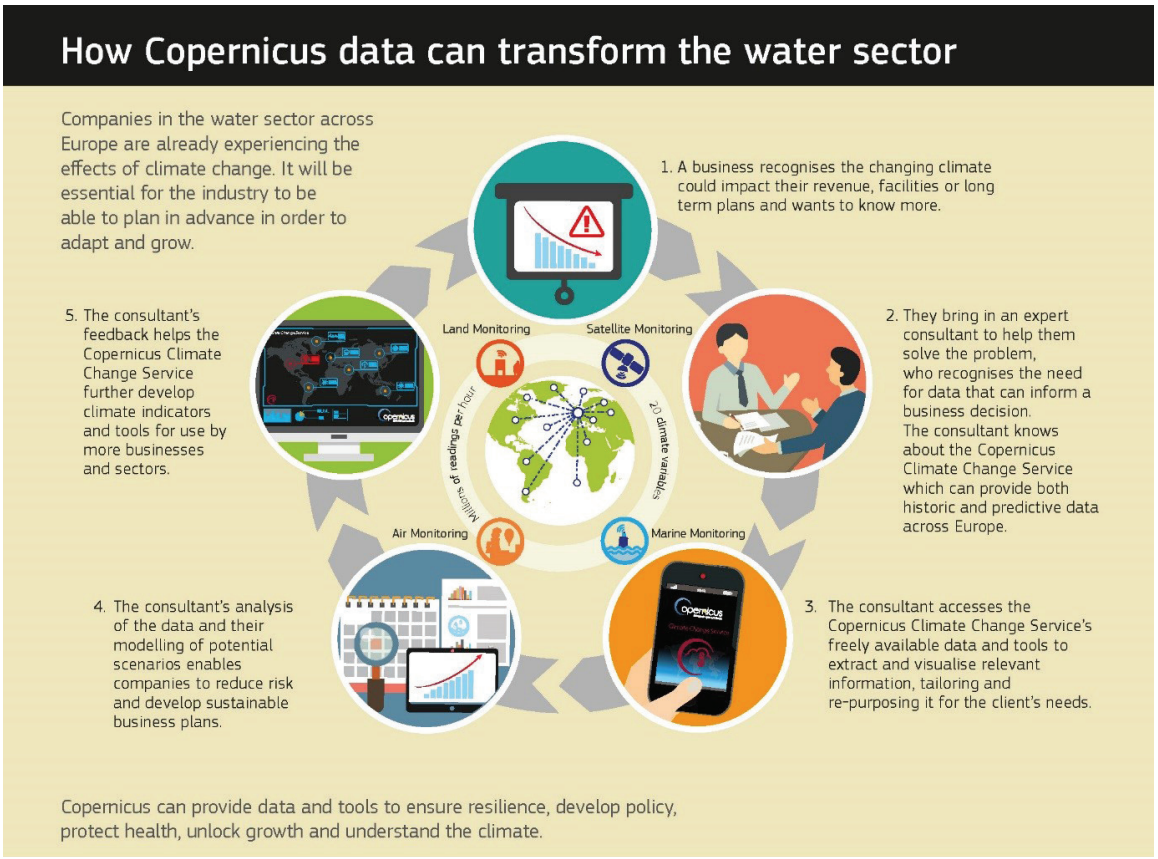

Hackathon aims to improve Global Flood Awareness System

FLORIAN PAPPENBERGER, FLORIAN RATHGEBER

A meeting to improve the Global Flood Awareness System (GloFAS) through collaborative computer programming took place at ECMWF on 16 and 17 January. The 'hackathon' brought together more than 60 participants from research organisations, universities and industry. They worked on new ways to visualise GloFAS data, to make GloFAS more accessible and to create new downstream applications and products based on GloFAS data.

Global toll

Flooding has the highest frequency of occurrence of all types of natural disasters across the globe, accounting for 39% of all natural disasters since 2000. Flood events affect millions of people every year through displacement from homes, unsafe drinking water, destruction of infrastructure, and injury and loss of life. On average, each year more than 5,500 people are killed by floods and more than 94 million people are affected worldwide. Producing global forecasts of flood events has only become possible in recent years, due to the emergence of new developments and capabilities of forecasting systems; the integration of meteorological and hydrological modelling capabilities; improvements in data, satellite observations and land surface hydrology modelling; and increased resources and computer power.

Funding for global flood forecasts is limited, and GloFAS has essentially been created through the volunteer enthusiasm of a few individuals. Although we can now produce these forecasts, there is still a long way to go to make them usable, in particular for NGOs. The GloFAS system is currently used in a pilot project by the International Red Cross for forecast-based finance. The project recognises that, while forecasts may be available, there is often no humanitarian organization ready to act before a disaster strikes. Such anticipatory action can be far more effective than a post-disaster response. The pilot project will disburse humanitarian funding as soon as a forecast threshold is crossed and before a potential disaster occurs. However, for such projects to work, the system needs to be accessible to and usable by a wide range of individuals.

Tools that could save lives

The hackathon, organised by ECMWF and JRC staff in their spare time, took the form of a competition to help address these issues of accessibility and usability. After an introduction to GloFAS and brainstorming around challenges that need to be addressed, the participants were free to form teams and formulate a problem that could be solved within the available time. Five teams entered the competition and set out to create a prototype that would impress the judges in terms of its technical solution, its wow factor and innovation. The three winning entries were:

- LIVE (Logistic and Infrastructure Visual Evaluation): Using GloFAS forecast information to create a 'Time to respond' map. Sets out to summarise GloFAS forecast information into a 'Time to respond' prioritisation map that helps decision-making before and during a flood emergency. This is presented in a user-friendly way with key statistics which could support decision-making.
- FloodIT: Integrates (client-side) the GloFAS output with a higher-resolution Digital Elevation Model (DEM) map, increasing granularity of information for local areas. It provides more intuitive information based on the GloFAS output to help local users understand their situation.
- Interception – A Flood Awareness Education Platform: An educational game/online interactive platform to help inform people about what they should be doing when a flood watch/warning alert is issued in their region. The game/platform will also educate them on what to do during and after a flood event.

The #FloodHack page on ECMWF's website has links to all the entries, along with photos from the weekend: http://tiny.cc/floodhack.

GloFAS hackathon at ECMWF. The event took the form of a competition to improve the accessibility and usability of GloFAS. (*Photo: Florian Rathgeber*)

A big thank you to all participants who made this #FloodHack such a great success and who contributed with their ideas and skills to further improve GloFAS.

The #Floodhack was supported by the Copernicus Emergency Management Service – Early Warning Systems and the EarthServer-2 project (H2020, grant agreement No 654367).

ECMWF and GloFAS

ECMWF is developing the Global Flood Awareness System (GloFAS) in co-operation with the European Commission's Joint Research Centre (JRC) and the University of Reading. GloFAS combines the Centre's medium-range weather forecasts with a hydrological model to provide global forecasts of flood events. GloFAS users include national and regional water authorities, water resource managers, hydropower companies, civil protection and first line responders, and international humanitarian aid organisations.

'Training the trainer' in the use of forecast products

ANNA GHELLI (ECMWF), **IGOR KOS** (Croatia Control Limited)

An in-depth understanding of ECMWF's products, in particular of ensemble forecasts, is essential for users to be able to integrate these products into their daily routines. This requirement is the driving force behind the high demand for ECMWF's course on the 'Use and Interpretation of ECMWF Products'. ECMWF has responded to this demand in various ways: increasing the number of courses, introducing blended courses (self-learning and face-to-face sessions) and providing webinars on specific topics. This year we have introduced a version of the course 'Use and Interpretation of ECMWF Products' targeting trainers and training champions. The idea is to help participants spread knowledge on how to get the most out of ECMWF products, by using their organisations' own channels of training.

The 'train the trainer' version, which took place from 1 to 5 February 2016, included many of the course's regular topics: there were sessions on data assimilation, forecasting extreme events, and satellite observations. The real novelties were the use of games to teach some basic ensemble forecasting concepts and the analysis of competencies needed to use ensemble forecast products effectively in daily forecasting tasks.

The idea of using games in education and training is not new. The 'gamification' of learning is an educational approach to motivate students to learn while using game elements in the learning environment. At ECMWF we have used simple games in courses in the past, and this year we have introduced a new game called 'How much are you willing to pay for a forecast?'. The game was developed jointly by scientists at ECMWF, IRSTEA (Institut national de recherche en sciences et technologies pour l'environnement et l'agriculture), the Red Cross/Red Crescent Climate Centre and UNESCO-IHE (Institute for Water Education).

Course participant David Jameson is an operational meteorologist at Wattisham Airfield in Suffolk, employed by the UK Met Office. He chiefly uses ECMWF's medium-range and long-range products to provide forecasts for the armed forces at the Airfield.

"The sessions on training were very useful. They highlighted current gaps in training and ways to address them," he said. *"We also played games, which we may be able to reuse in the training we provide."*

The participants considered that mastering ensemble forecast products and more generally probability forecasts is critical for the success of a weather service. The analysis of gaps in training revealed that we have some more work to do to improve understanding of ensemble products, especially for severe events.

One of the participants, Nataša Strelec Mahović, is the head of the Weather Analysis and Forecast Department in the Meteorological and Hydrological Service of Croatia (DHMZ). In this capacity, she is also in charge of training forecasters.

"The training-related sessions will be useful to provide forecasters with more focussed and more formal training on ensemble products," Dr Strelec

Ensemble forecasts 'critical'. As the scatter graph shows, all participants considered that ensemble forecast products are 'critical' to the success of organisations, but some only felt moderately confident in using them.

Mahović said. "*It emerged that all course participants are aware of the importance of using ensemble products, but there was quite a spread in how good people feel they are at using them.*"

The World Meteorological Organization has developed competency frameworks for a number of meteorological areas. The course was a good opportunity to look into the competencies needed to use ensemble forecast products effectively. Working in groups, the participants produced the following list of competencies:

- Discover and select appropriate products depending on the weather event
- Link global scenarios with their associated probabilities to local weather making use of the full ensemble distribution
- Assess flow predictability
- Get to know your end users, create tailored products and communicate effectively
- Provide feedback to NWP data producers

These competencies will serve as feedback for future competency frameworks for forecasters as well as an inspiration for the work done in ECMWF's Member and Co-operating States. Course participant Igor Kos, a trainer at Croatia Control Ltd (CCL, Croatia's official provider of aviation meteorological services), presented the competency activity carried out during the course at a Competency Assessment Workshop hosted by his company. The workshop focused on competencies and competency assessment for Aeronautical Meteorological Personnel (AMP). In his presentation, Igor emphasised the importance of group work and how discussions among experts can lead to the production of a relevant list of competencies. The workshop highlighted the importance of defining competencies and how competency frameworks are critical to the success of organisations.

Roll the dice. Course activities included two games on using probability in decision-making processes.

ECMWF NEWSLETTER GOING DIGITAL

As part of our aim to reduce our carbon footprint, we would like to encourage our readers to access the digital version of the ECMWF Newsletter.

Newsletters are already available as PDF documents here: *www.ecmwf.int/en/about/news-centre/media-resources*

This issue will be the first to be made available in fully digital, smartphone-friendly form, with each article as a web page.

If you would like to be notified when the ECMWF Newsletter is available online, please contact us at *newsletter@ecmwf.int* and ask to be added to our email alerts list. Please use the same email address to let us know if you no longer require the print edition of the Newsletter.

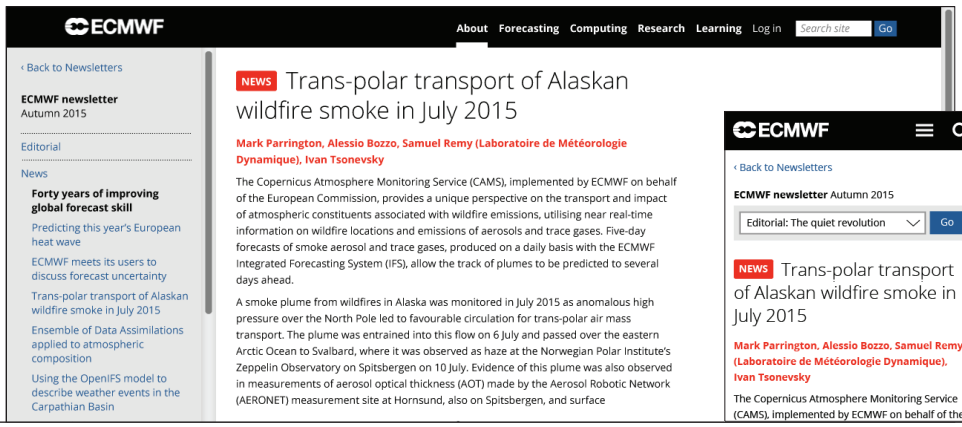

Digital Newsletter. Article diplay and navigation will vary according to the device used, as shown here for desktops and smartphones.

New model cycle brings higher resolution

ELÍAS HÓLM, RICHARD FORBES, SIMON LANG, LINUS MAGNUSSON, SYLVIE MALARDEL

On 8 March 2016, ECMWF introduced a new model cycle of the Integrated Forecasting System (IFS) into operations. Cycle 41r2 represents a significant step forward in accuracy and resolution and, at a grid spacing of 9 km, it is currently the highest-resolution global forecasting system in the world. The main change is an increase in horizontal resolution in most parts of the forecasting system. For high-resolution forecasts (HRES) and ensemble forecasts (ENS) the grid-point resolution is roughly doubled to 9 km and 18 km, respectively, while for the Ensemble of Data Assimilations (EDA) it is tripled to 18 km. In combination with several other scientific and technical changes, this has led to a significant increase in forecast accuracy and computational efficiency. This article sets out the main changes leading to improvements in forecast quality.

Resolution increase and new grid

The 2016 horizontal resolution upgrade is designed to achieve a balance between greater resolution and increased forecast accuracy on the one hand and computational cost on the other. A number of combinations of horizontal resolutions were tried for 4DVAR, EDA, HRES and ENS. The solution that was eventually adopted is summarised in Table 1.

The main innovation in the resolution upgrade is the introduction of a new 'cubic octahedral' grid (with new prefix 'O' to distinguish it from the reduced Gaussian grid with prefix 'N'). The cubic octahedral grid is based on a cubic spectral truncation and a new mesh that allows for the future implementation of a hybrid spectral/grid-point model. The new grid is described in detail in *Malardel et al.* (2016). The change from the current linear (TL) to a cubic (TC) spectral truncation means that the shortest resolved wave is represented by four rather than two grid points. This change was made because in the IFS a cubic grid leads to more accurate forecasts than a linear grid at the same computational cost. The cubic octahedral grid, denoted by TCo, increases the resolution in grid-point space somewhat less and is 25% less costly than a TC grid at the same spectral truncation.

The benefits of the cubic grid can be seen in increased realism at smaller scales, where less diffusion is needed than for a linear grid, and where there is no need for a dealiasing filter because now four points represent the shortest wave. The efficiency of representation of the kinetic energy spectrum (Figure 1) is significantly improved, with more energy in the smaller scales due to a reduction of the diffusion and the removal of the dealiasing filter. There is also consistency between the analysis and forecast spectra, which was not the case with the linear grid, where the analysis trajectory required stronger diffusion than the forecast.

The improved consistency between analyses and forecasts in 41r2 can be seen in Figure 2, where the level of detail in

Average grid spacing	HRES	ENS		4DVAR inner loops			EDA		
		Medium-range	Monthly extension	1st	2nd	3rd	Outer	1st	2nd
128 km								TL159	TL159
				TL255	TL255	TL255		TL191	TL191
64 km			TL319		TL319				
						TL399	TL399		
32 km		TL639	TCo319						
16 km	TL1279	TCo639					TCo639		
9 km	TCo1279								

Table 1 The new model cycle brings a number of resolution upgrades across the forecasting system. The table shows the changes from Cycle 41r1 (blue) to Cycle 41r2 (red). TL stands for triangular-linear and TCo for triangular-cubic-octahedral. The numbers indicate the spectral truncation.

2-metre temperature is very similar in the 41r2 analysis and forecast, whereas the analysis in 41r1 is smoother than the 41r1 forecast. The increased level of small-scale detail going from 41r1 to 41r2 is also visible.

In general the increased resolution leads to a better representation of coastlines and orography with consistent gains in forecast performance in the tropics and extra-tropics for 2-metre temperature, 2-metre humidity, and 10-metre wind speed. There is also a substantial reduction in localised (unrealistic) precipitation extremes over orography. This is achieved by the cubic grid representation and modifications in the semi-Lagrangian advection scheme, as described by *Malardel et al.* (2016).

Data assimilation and ensemble forecasts

There are several further improvements in consistency within and between the different forecasts and analyses. Increasing the ensemble forecast and EDA resolution to TCo639, which is 18 km in grid-point space, brings both close to the 16 km resolution of the previous high-resolution forecast. In addition to improved overall ensemble forecast scores, the higher resolution also leads to improved analyses and forecasts of tropical cyclones. The tracks and in particular the intensity of tropical cyclones are now more accurate due to the increased resolution, which enables more accurate modelling of smaller and deeper tropical cyclones. This can be seen in Figure 3, which shows that forecasts of the core pressure of tropical cyclones have become more accurate (smaller root-mean-square error) while the spread has increased, which improves the forecast reliability.

The resolution increase of the analysis increments of 4DVAR ('inner loops') to TL399 is the second main factor – after the forecast resolution increase – responsible for the overall improvement in forecast skill. The combination of higher-resolution forecasts and inner loops results in a closer fit between measurements and the model, which enables

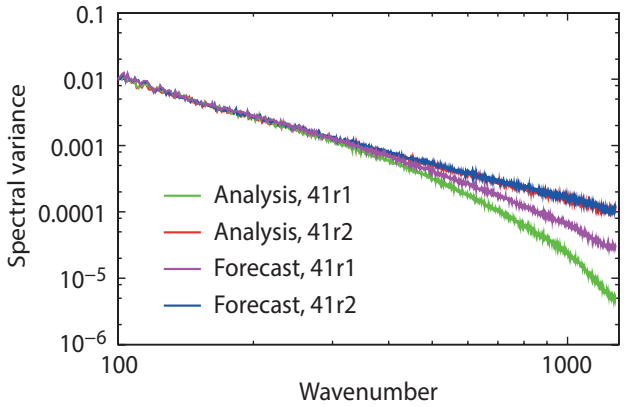

Figure 1 Spectra of kinetic energy at model level 137, the level closest to the surface, shown for HRES analyses and 24-hour forecasts.

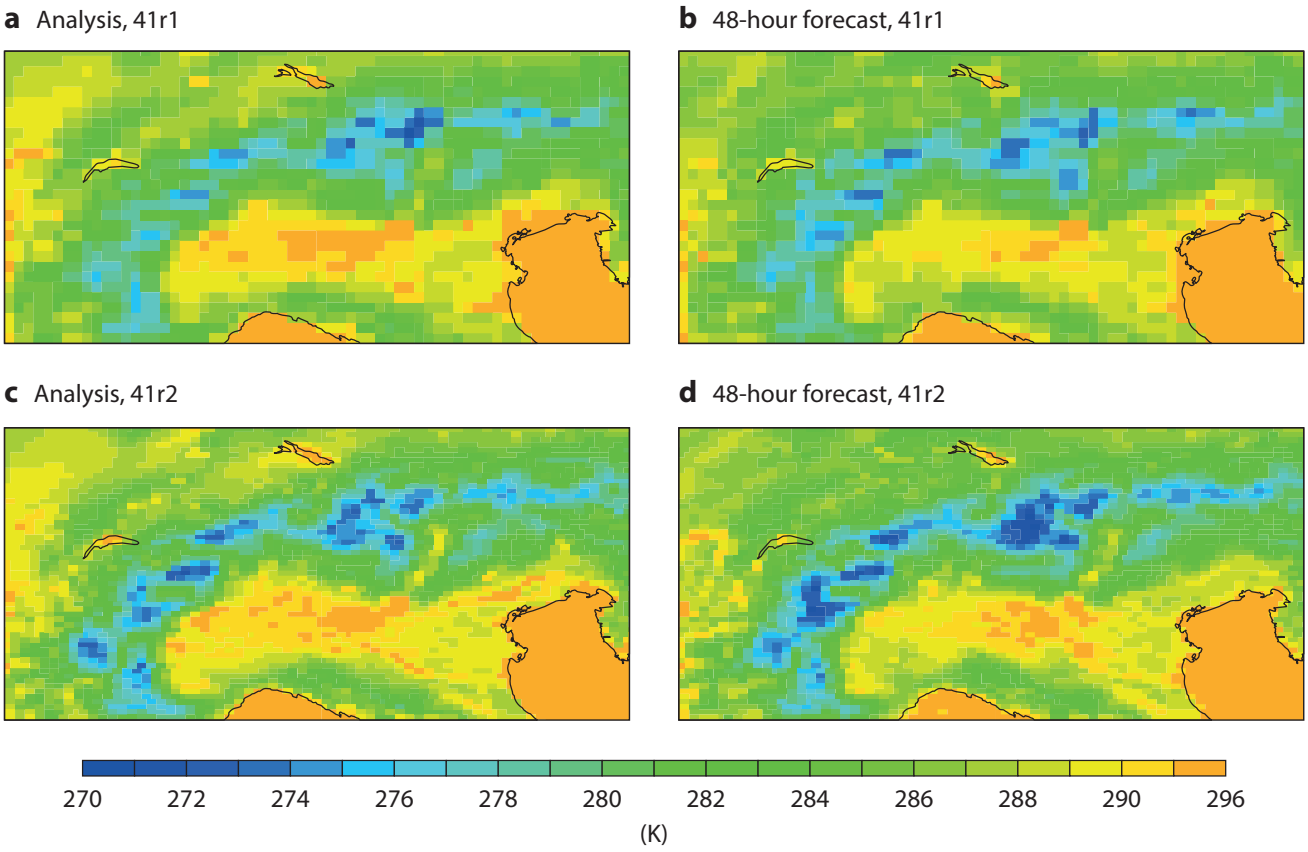

Figure 2 Two-metre temperature valid on 1 June 2015 00 UTC for (a) 41r1 analysis, (b) 41r1 HRES 48-hour forecast, (c) 41r2 analysis and (d) 41r2 HRES 48-hour forecast.

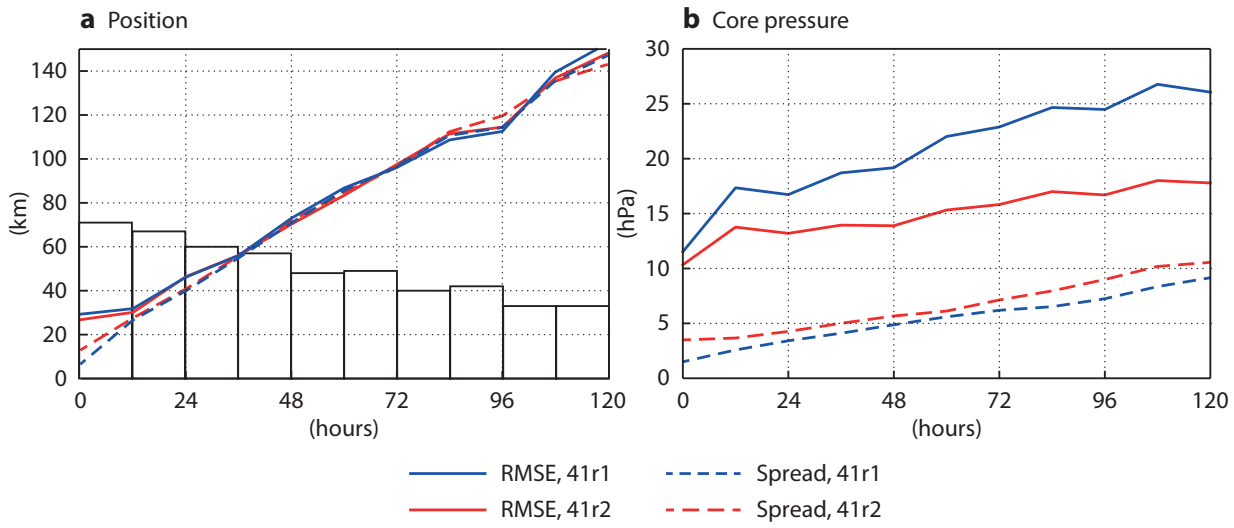

Figure 3 Root-mean-square error (RMSE) and spread of ensemble forecasts of tropical cyclone track and intensity for 45 initial dates in total from June to July 2015, showing (a) position error and spread and (b) core pressure error and spread. The sample size, indicated by the bars in (a), starts from 70 at 0 hours and reduces gradually to half that number at 120 hours.

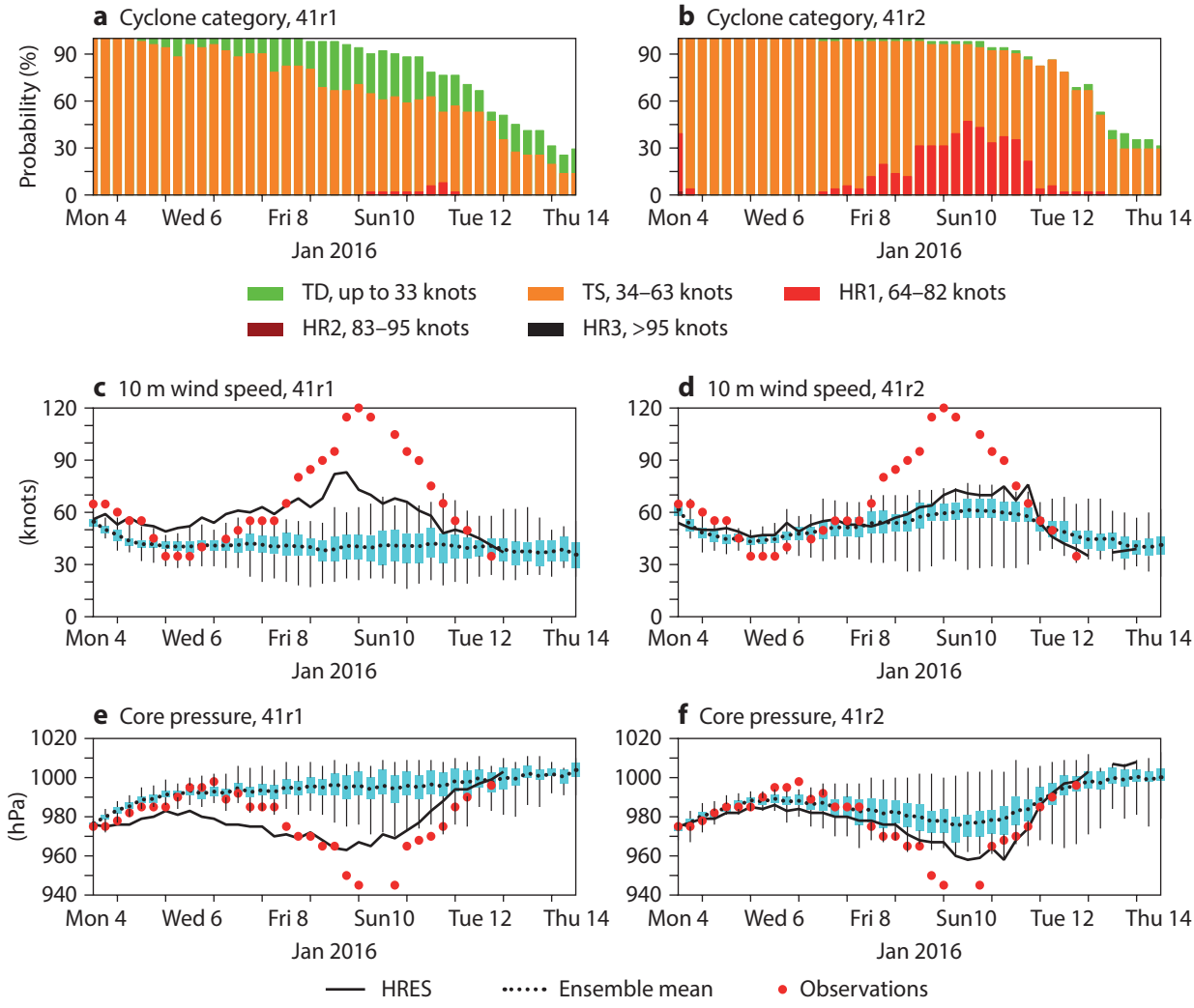

Figure 4 Forecasts for tropical cyclone Ula showing the ENS probability of Ula falling into different strength categories for (a) Cycle 41r1 and (b) Cycle 41r2; ENS and HRES 10-metre wind speed for (c) Cycle 41r1 and (d) Cycle 41r2; and ENS and HRES mean sea level pressure in the cyclone centre with observations for (e) Cycle 41r1 and (f) Cycle 41r2.

a better use of space-based and in-situ high-resolution observations. The increased resolution of the analysis increments also enables corrections at smaller scales. For Cycle 41r2, most of the systematic tests of different inner-loop options used linear grids. The best compromise between computational cost and forecast accuracy was achieved by a 4DVAR with three inner loops with resolution TL255 followed by TL319 and TL399. Cubic-octahedral inner loops will be considered for later cycles.

The improvement in ensemble forecasts depends on the complex interaction between ENS, EDA and HRES, because the ENS initial state includes improved EDA forecasts centred on improved HRES analyses. This can be illustrated by looking at a typical tropical cyclone case, Ula in Figure 4, which shows 10-day ensemble and high-resolution forecasts from before (41r1) and after (41r2) the resolution increase. As in the averages in Figure 3, the ensemble members are now closer to observations, with a larger fraction of category HR1 cyclone forecasts, while at the same time the ensemble spread is larger. Another improvement in this case is that the high-resolution forecasts mostly fall within the spread of the ensemble, because on the one hand the spread has become a better estimate of the error (Figure 3) and on the other both HRES and ENS have become more accurate and thus closer to each other. At the start of the forecast, the spread is also larger due to the higher EDA resolution. The improvements in the EDA error and spread are even greater than for other parts of the system because the EDA grid-point resolution has more than tripled.

The consistency in ENS was also improved by moving the step-decrease in resolution of the forecast (going from 'medium-range' at TCo639 to 'monthly extension' at TCo319) from day 10 out to day 15, thus ensuring consistent high forecast resolutions throughout the medium range to 15 days. This can be seen in the 2-metre temperature Continuous Ranked Probability Score (CRPS) in Figure 5, where in addition to the improved scores for Cycle 41r2, the jump to less accurate forecasts at day 10 seen in Cycle 41r1 is moved to day 15, where it affects forecast accuracy less because the errors at day 15 are larger.

Other selected changes

While most of the average improvements in scores come from the increases in resolution – in particular in the forecast resolution and the 4DVAR inner-loop resolution – several other changes to the model have reduced specific systematic forecast errors.

The stability of the semi-Lagrangian numerical scheme near strong wind gradients has been improved, reducing noise downstream of significant orography and in tropical

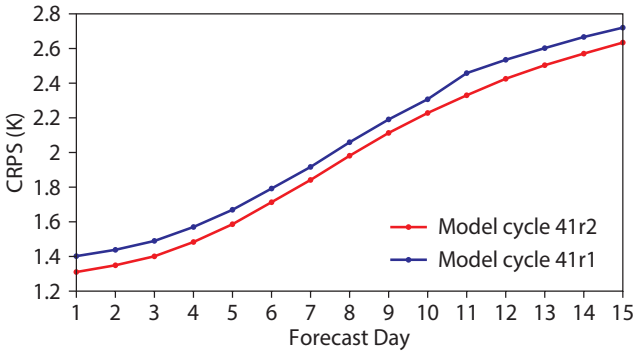

Figure 5 Continuous Ranked Probability Score (CRPS) for ensemble forecasts of 2-metre temperature in Europe averaged over 12 UTC forecasts from 10 August 2015 to 25 February 2016.

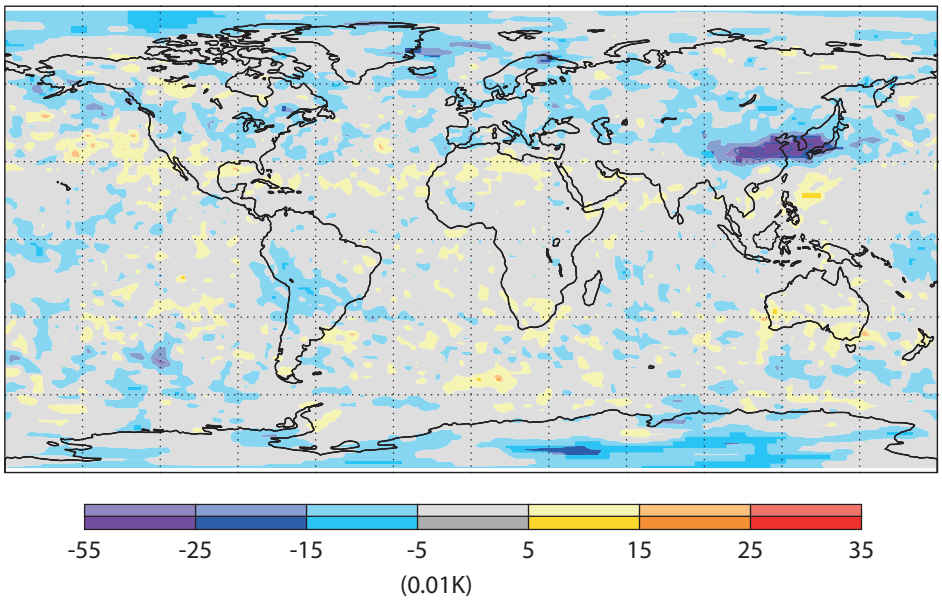

Figure 6 Reduction of 200 hPa temperature day 2 RMSE in HRES forecasts for December/January/February 2015–16 resulting from changes to the semi-Lagrangian advection scheme. Saturated colours denote a significance level of 5%.

HRES 41r2 score card

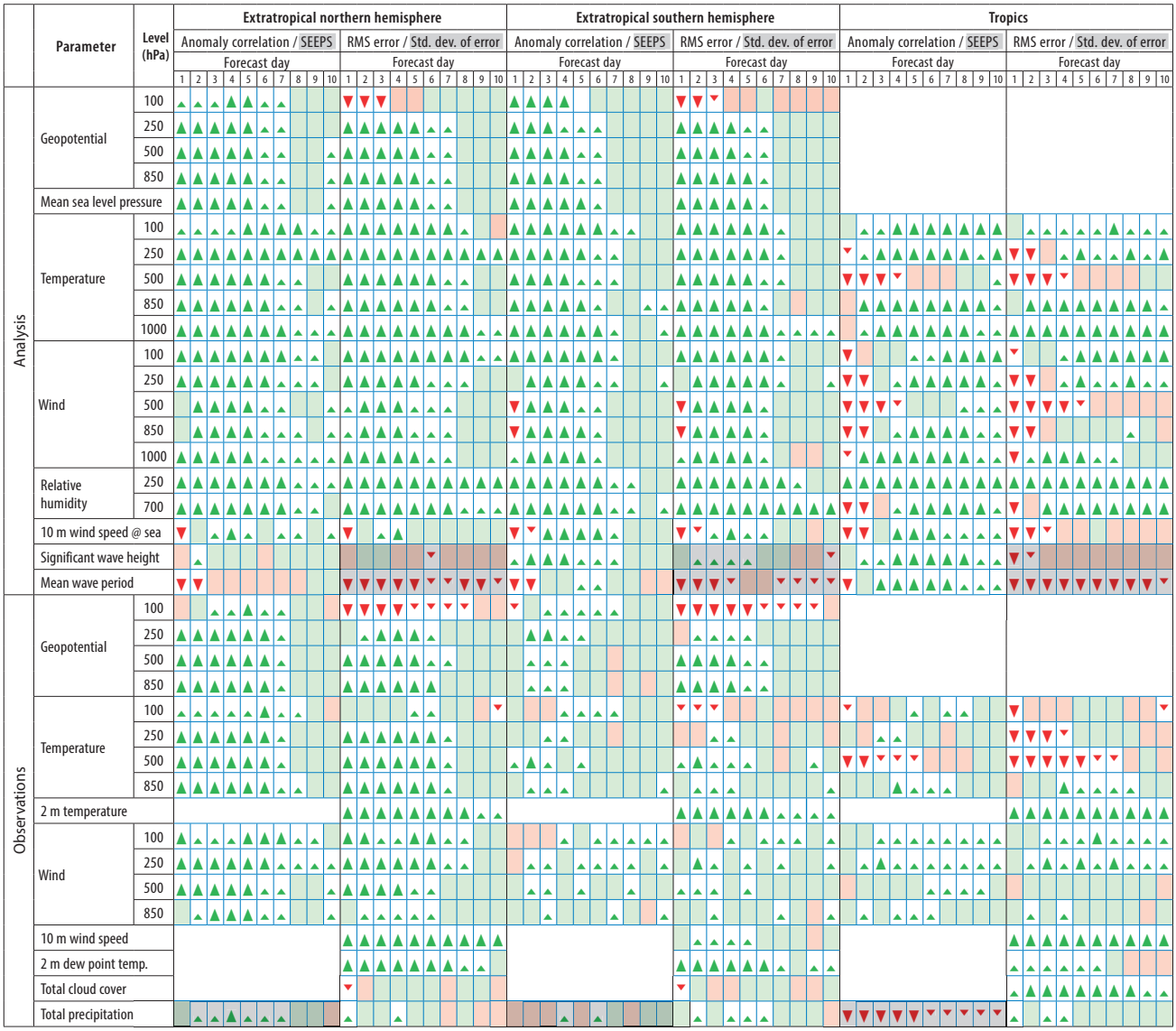

ENS 41r2 score card

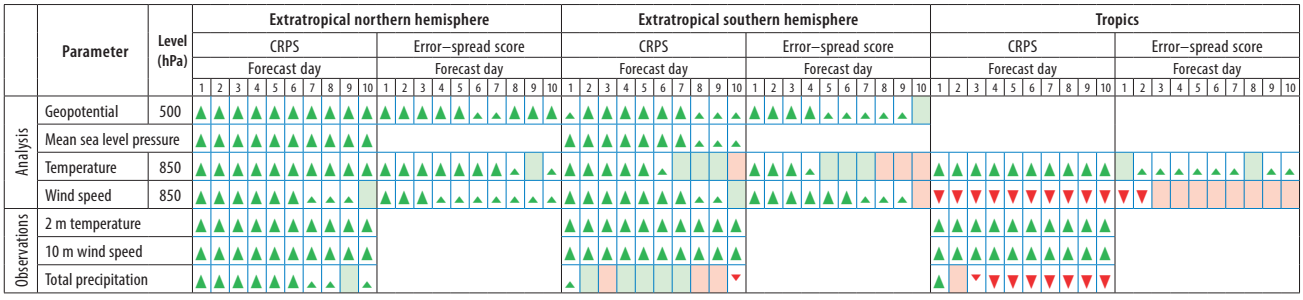

Symbol legend: for a given forecast step...

- Cy41r2 better than Cy41r1 – statistically highly significant
- Cy41r2 better than Cy41r1 – statistically significant
- Cy41r2 better than Cy41r1 – not statistically significant
- Little difference between Cy41r2 and Cy41r1
- Cy41r2 worse than Cy41r1 – not statistically significant
- Cy41r2 worse than Cy41r1 – statistically significant
- Cy41r2 worse than Cy41r1 – statistically highly significant

Figure 7 Score card for Cycle 41r2 HRES and ENS versus Cycle 41r1 verified by the respective analyses and observations at 00 and 12 UTC for 211 days in the period 10 August 2015 to 7 March 2016.

cyclones, and leading to significantly better upper-air forecasts over East Asia, as seen in the lee of the Himalayas in Figure 6 (*Diamantakis & Magnusson*, 2015).

The modelling of radiative heating/cooling at the surface has been improved by introducing approximate updates on the full grid at every time step. This has led to a reduction in 2-metre temperature errors (Figure 5), particularly near coastlines in places where surface conditions vary abruptly, as described in greater detail by *Hogan & Bozzo* (2015).

The use of satellite data has also been improved, which has led to improvements in specific areas. For example, microwave data is used in more challenging situations, such as mountain areas and snow-covered land surfaces, and coverage of satellite-derived winds is improved in the mid-latitudes.

Overall improvements

An overview of scores for high-resolution and ensemble forecasts is shown in Figure 7. The performance of both HRES and ENS is improved throughout the troposphere. Error reductions in the order of 2–3% (root-mean-square error and CRPS, respectively) are found for most upper-air parameters and levels. This corresponds to an increase of about 2 hours in the lead time at which the primary headline score for HRES – the 500 hPa geopotential anomaly correlation – drops below 80%. There is an even larger lead time gain for some near-surface parameters, such as a gain of more than 12 hours in ensemble forecasts for 2-metre temperature over Europe, as shown in Figure 5. This is mostly the result of a local reduction in errors in coastal areas with a large land–sea contrast.

Improvements are seen in verification both against the model analysis and against observations. In the tropics, evaluation against model analysis shows an apparent degradation in the short and near-medium range, mostly due to a more active analysis resulting from the increase in resolution of the EDA. Verification against observations, however, gives neutral to positive results in the tropics, except for temperature at 500 hPa and above, which shows a slight degradation. Further improvements to the EDA background error calculation are expected to resolve this in the next operational cycle. There is a small (0.2 K) mean cooling in upper troposphere forecasts. This shows up as an increased root-mean-square error (RMSE) for geopotential at 100 hPa because the mean geopotential in the lower stratosphere is sensitive to changes in the vertically integrated tropospheric temperature. The increased variability of the higher-resolution model also shows up as an apparent degradation in some parameters, for example in waves and precipitation in the tropics.

Summary

Cycle 41r2 has improved the accuracy and consistency of the different components of the IFS, leading to error reductions of 2–3% in tropospheric forecasts. The increase in resolution of the EDA and ENS to 18 km has led to increased realism in the representation of smaller-scale features, such as tropical cyclones, and increased consistency with HRES, which is now the highest-resolution global forecasting system in the world. Several long-standing systematic errors have been reduced through improvements in the model and better use of satellite data, in particular in coastal areas. All these improvements in forecast skill will help forecasters, who will benefit even more once their systems have been adapted to take advantage of the higher-resolution fields.

The work towards IFS Cycle 41r2 achieved a good balance between higher resolution, increased forecast accuracy and affordable computational cost. This was made possible only through intense collaboration involving all parts of ECMWF, including upgrades and optimizations to computing capabilities and supporting software as well as the IFS, together with extensive testing and evaluation.

FURTHER READING

Diamantakis, **M.** & **L. Magnusson**, 2015: Numerical sensitivity of the ECMWF model to Semi-Langrangian departure point iterations. ECMWF Research Department *Technical Memorandum* **No. 768**.

Hogan, **R.** & **A. Bozzo**, 2015: Reducing surface temperature errors at coastlines. *ECMWF Newsletter* **No. 145**, 30–34.

Hólm, **E.**, **M. Bonavita** & **L. Magnusson**, 2015: Improved spread and accuracy in higher-resolution Ensemble of Data Assimilations. *ECMWF Newsletter* **No. 145**, 15.

Malardel, **S.**, **N. Wedi**, **W. Deconinck**, **M. Diamantakis**, **C. Kühnlein**, **G. Mozdzynski**, **M. Hamrud** & **P. Smolarkiewicz**, 2016: A new grid for the IFS. *ECMWF Newsletter* **No. 146**, 23–28.

Siemen, **S.**, **I. Russell**, **T. Quintino** & **D. Varela Santoalla**, 2016: Software updates in preparation for model cycle 41r2. *ECMWF Newsletter* **No. 146**, 16.

Use of high-density observations in precipitation verification

THOMAS HAIDEN, SINÉAD DUFFY

Verification of forecasts against surface observations from SYNOP stations is an important part of monitoring progress in numerical weather prediction systems such as ECMWF's Integrated Forecasting System (IFS). Parameters observed at such stations typically include 2-metre temperature and humidity, 10-metre wind, total cloud cover and precipitation. In addition to SYNOP observations, which are distributed via the Global Telecommunication System (GTS), many countries maintain higher-density national observational networks which provide data that is not generally available on the GTS. In 2014 ECMWF started an initiative to collect such observations from its Member and Co-operating States for use in model evaluation. Based on the experience gained in previous efforts (*Csima & Ghelli*, 2008), it was decided to use a unified data format for the data transfer in order to facilitate its long-term maintenance.

Data from additional stations improves the sampling of the quantity to be evaluated. First results obtained from the use of precipitation data in forecast evaluation show that this leads to reduced noise in time series of forecast skill. It also increases confidence in comparisons between operational and experimental model cycles, which are necessarily based on a limited verification period. In the case of precipitation and wind, the fact that less frequent, higher-intensity events are of special interest adds to the value of a dense observation network.

Collection of high-density observations in Europe

As of February 2016, ECMWF receives high-density observations (HDOBS) of precipitation on a regular basis from a number of Member and Co-operating States. Some countries additionally provide observations of surface parameters such as 10-metre wind speed and 2-metre temperature. The temporal aggregation of the precipitation data varies between 1-hourly and 24-hourly. For verification purposes it is being aggregated into 6-hour and 24-hour totals. The ratio of the number of HDOBS to SYNOP stations varies between countries and typically lies between 2/1 and 3/1. Figure 1 shows how the total number of HDOBS stations included in the initiative has increased considerably between November 2014 and January 2016.

Reduction of verification uncertainty

The skill in predicting heavy precipitation is important for many forecast users. As documented by *Forbes et al.* (2015), heavy precipitation forecasts have improved over the last decade due to upgrades to the IFS, in particular the representation of cloud and precipitation physics. However, when high thresholds of precipitation are evaluated, the detection of longer-term trends is made difficult by the noise associated with small sample sizes and considerable inter-annual variability. This is especially true for longer lead times, where individual events are captured less consistently. Figure 2 illustrates this for the difference in the Symmetric Extremal Dependence Index (SEDI) (Box A) between the high-resolution forecast (HRES) and forecasts from the ERA-Interim reanalysis at forecast days 1, 5, and 10, based on the verification of 24-hour precipitation against SYNOP for the European domain. Although only a moderately high threshold of 20 mm is used, and 12-month running averages are shown, the scores exhibit considerable inter-annual variability at forecast days 5 and 10. This makes it more difficult to quantify the effect of model improvements at these time ranges.

Skill Scores

A

SEDI

The Symmetric Extremal Dependence Index (SEDI) is a skill score appropriate for extreme events. It provides meaningful results in the case of rare events where the hit rate and false alarm rate decrease towards zero. It is defined for a binary event and thus requires a threshold to be set.

TS and ETS

The Threat Score (TS) is a skill score for binary events and requires a threshold to be set. It is defined as the ratio of the number of hits to the sum of hits, false alarms and misses. The Equitable Threat Score (ETS) is an adjusted Threat Score in which the number of hits that would be expected to occur by chance alone is deducted from the number of hits.

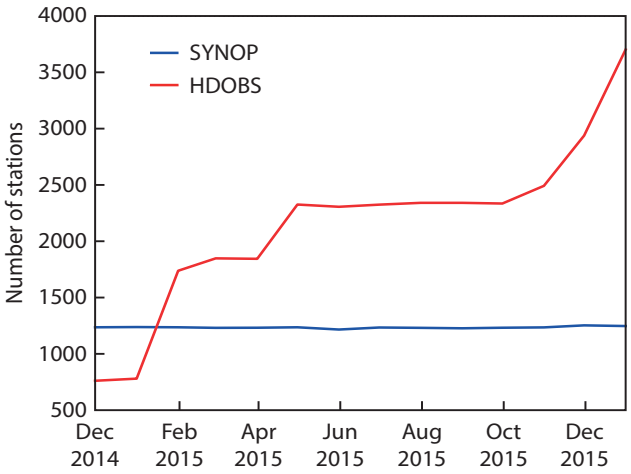

Figure 1 Evolution of the number of high-density observation (HDOBS) stations included in the HDOBS initiative, compared to the total number of SYNOP stations in the same countries, showing the effect of more Member and Co-operating States joining the initiative in 2015 and early 2016.

The time period covered by the HDOBS dataset is not yet long enough to provide improved estimates of long-term skill evolution. However, it also has a positive effect on the consistency of mean scores averaged over a limited period of time. Figure 3 shows the Equitable Threat Score (ETS) (Box A) of the operational high-resolution forecast (HRES) evaluated over a 13-month period using SYNOP and HDOBS. Although the two regions shown (Norway and Turkey) have quite different precipitation climates and processes, some aspects of the results are similar. In both areas, a reduction of noise in the curves can be seen for the highest threshold of 50 mm. For 10 and 20 mm, the verification against HDOBS largely confirms the dependence of skill on forecast range obtained from SYNOP. ETS values for 10 and 20 mm are surprisingly similar between the two regions in the medium forecast range around day 5 while in the short range the scores are somewhat higher for Norway. At 50 mm, there is a stronger drop in skill from day 1 to day 2 in the more convectively active area of Turkey compared to Norway, where the heaviest precipitation events are mostly due to orographic upslope effects, which are associated with higher predictability.

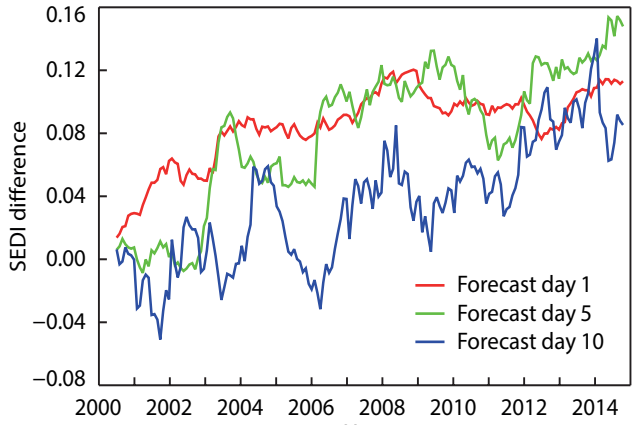

Figure 2 Evolution of 24-hour precipitation skill of the HRES relative to ERA-Interim for a threshold of 20 mm at forecast days 1, 5, and 10 based on verification against SYNOP, showing 12-month running averages.

Upscaling of observations

The mismatch in scale between the model grid and the point-like rain gauge observations can affect the quality of precipitation scores depending on how spatially representative the observations are. To eliminate this mismatch, observations have to be upscaled to the model grid. *Göber et al.* (2008) showed that without such upscaling a 'perfect' model, which in their case was constructed from grid-box averages of high-density observations, scored an Equitable Threat Score of only 0.5 for precipitation thresholds of 30 mm a day and higher, rather than the best possible value 1.0.

In practice, only part of the subgrid-scale variability of the precipitation field is known from observations, and the quality of the upscaling depends on the number of stations available within each grid box. From operational high-resolution (1 km) radar-plus-raingauge precipitation analyses provided by the Central Institute for Meteorology and Geodynamics (ZAMG, Austria) it was found that, at the previous HRES grid spacing of 16 km (reduced to 9 km in March 2016), having three stations instead of one per grid box reduces the effect of the scale mismatch on scores by more than a half. Even with high-density observations, the fraction of grid boxes on the IFS model grid which fulfil this condition is very small. For the area of Germany, for example, only 0.5% of grid boxes in the 16 km grid contain three or more stations. However, if the scale is increased to three times the grid spacing (about 50 km), this number increases to 54% (compared to 13% for SYNOP). Such upscaling, not just of observations but also of the forecast, is important to ensure that the verified quantity corresponds to the smallest scales actually resolved by the model.

Figure 4 shows how skill scores such as the Equitable Threat Score and the Symmetric Extremal Dependence Index increase when determined by verification against upscaled observations, as compared to the use of point values. The upscaling was performed by taking an average of all the observations in a grid box. Up to about 20 mm the increase in skill is due to reductions in both the number of missed events and false alarms. At higher thresholds, it is mainly

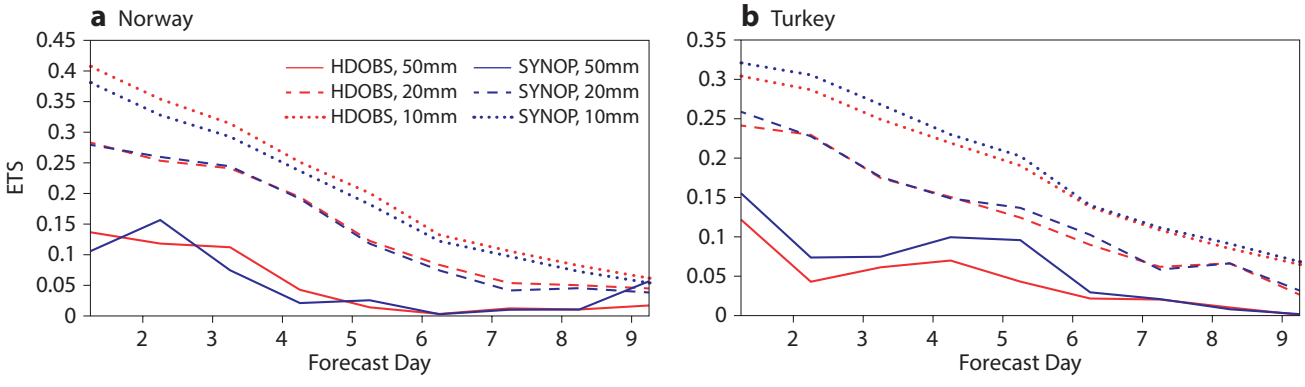

Figure 3 The Equitable Threat Score (ETS) in Norway and Turkey from SYNOP and HDOBS for precipitation events exceeding 10, 20, and 50 mm over 24 hours. The verification period is November 2014 to December 2015.

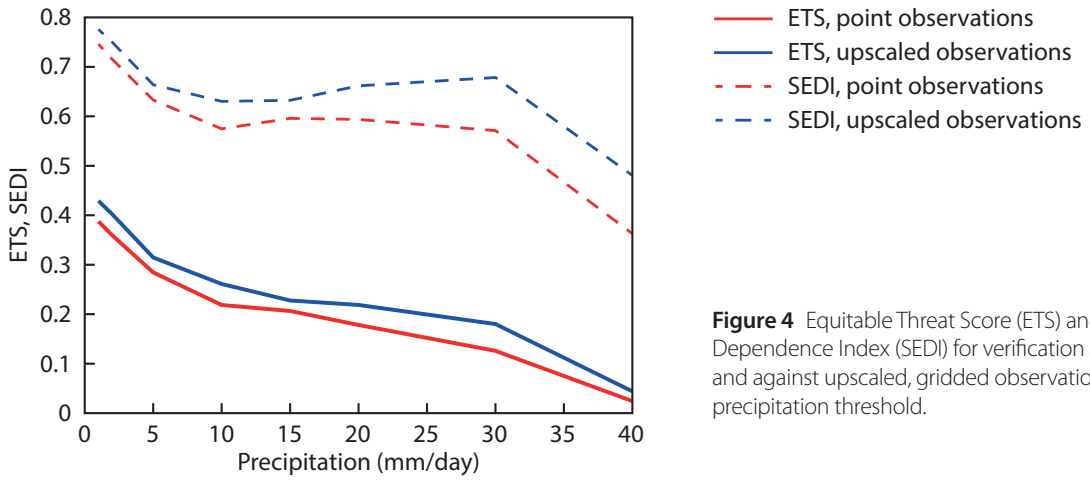

Figure 4 Equitable Threat Score (ETS) and Symmetric Extremal Dependence Index (SEDI) for verification against point values and against upscaled, gridded observations as a function of precipitation threshold.

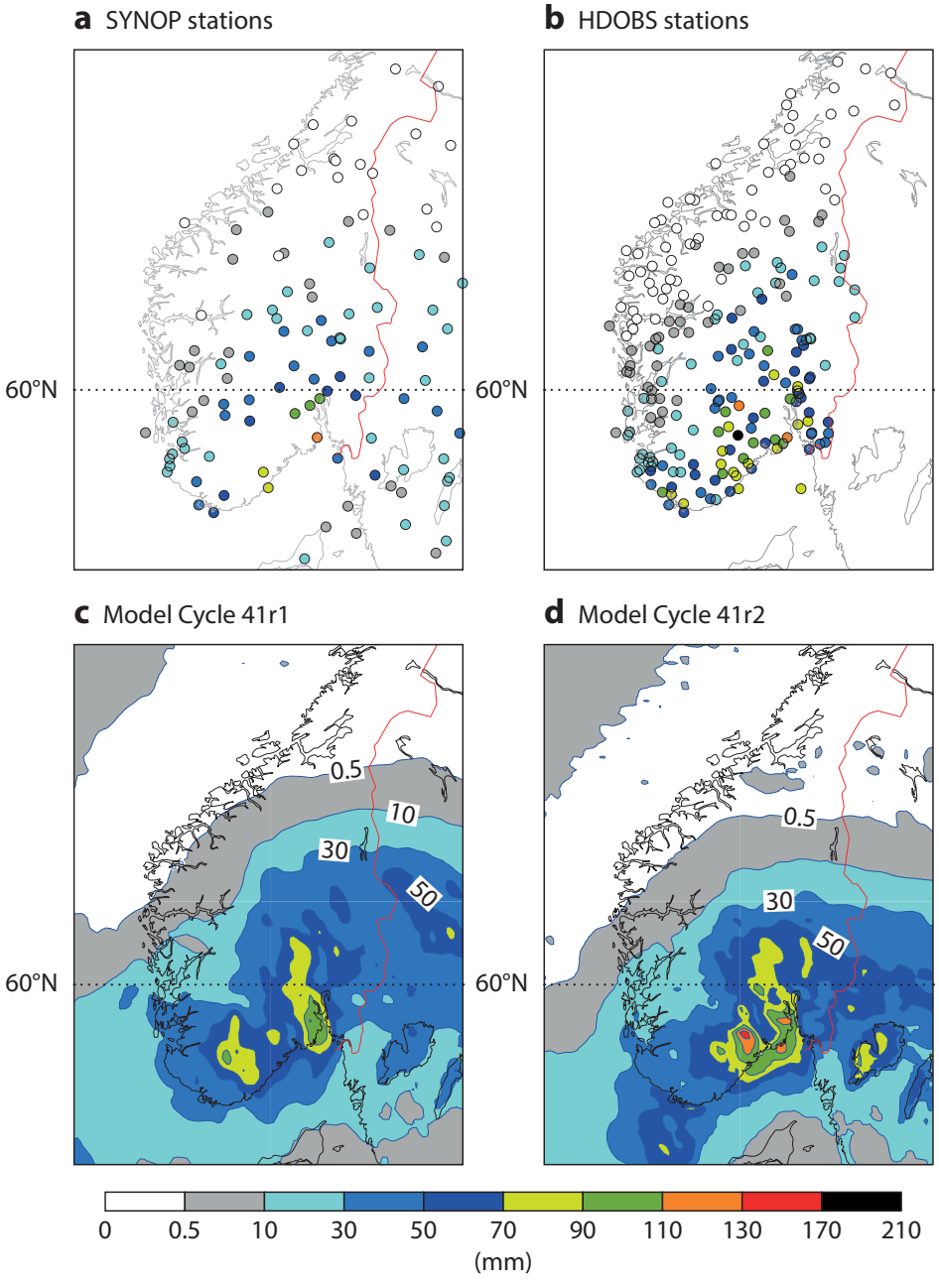

Figure 5 48-hour precipitation totals for the period 0600 UTC on 1 September to 0600 UTC on 3 September 2015 at (a) SYNOP stations and (b) HDOBS stations, and corresponding HRES forecasts for a lead time of 3 days (30 to 78-hour forecast) from (c) model cycle 41r1 and (d) model cycle 41r2.

due to fewer missed events. The upscaling reduces the influence on scores of the most localised events, where heavy precipitation is observed in one location but not at neighbouring stations. It increases the number of light to moderate precipitation events and reduces the number of heavy precipitation events. This effect increases with precipitation amount. For example, the number of events exceeding 20 mm is reduced by about 20%, the number of events exceeding 40 mm by about 50%.

Another way of addressing the scale disparity between precipitation forecasts and rain gauge observations has recently been proposed by Tim Hewson and Florian Pappenberger (personal communication) at ECMWF. They have shown that the estimation of point rainfall probabilities from the ensemble forecast can be improved by taking into account situation-dependent (e.g. convective/non-convective) subgrid-scale variability. Work at ECMWF on situation-dependent verification and post-processing is currently ongoing and may be extended to other parameters, such as 2-metre temperature, to elucidate situation-dependent model biases.

Case studies

High-density observations aid in the daily monitoring of forecast performance for high-impact weather. They provide improved estimates of the areal precipitation distribution in the most heavily affected areas. Apart from deep convection, strong gradients in the precipitation field often result from orographic effects, two examples of which are briefly described below.

Norway – September 2015

In the first two days of September 2015, the south of Norway experienced heavy precipitation associated with a cut-off low in the upper-level flow which became quasi-stationary over the North Sea. The centre of the associated surface low moved slowly over the course of several days from Denmark into southern Norway. The region had already experienced heavy rainfall a few days prior to the event and the ground was therefore pre-conditioned to produce a strong hydrological response. The event led to widespread flooding, landslides, the closure of roads and rail lines, and the closure of a runway at Oslo airport. The highest precipitation amounts were observed inland, some distance from the southeast-facing coast, with a maximum of 182 mm in 48 hours. The European Flood Awareness System (EFAS) run at ECMWF produced a number of flash-flood warnings in the area, as documented in the EFAS Bulletin August–September 2015, downloadable from the EFAS website (*www.efas.eu/*).

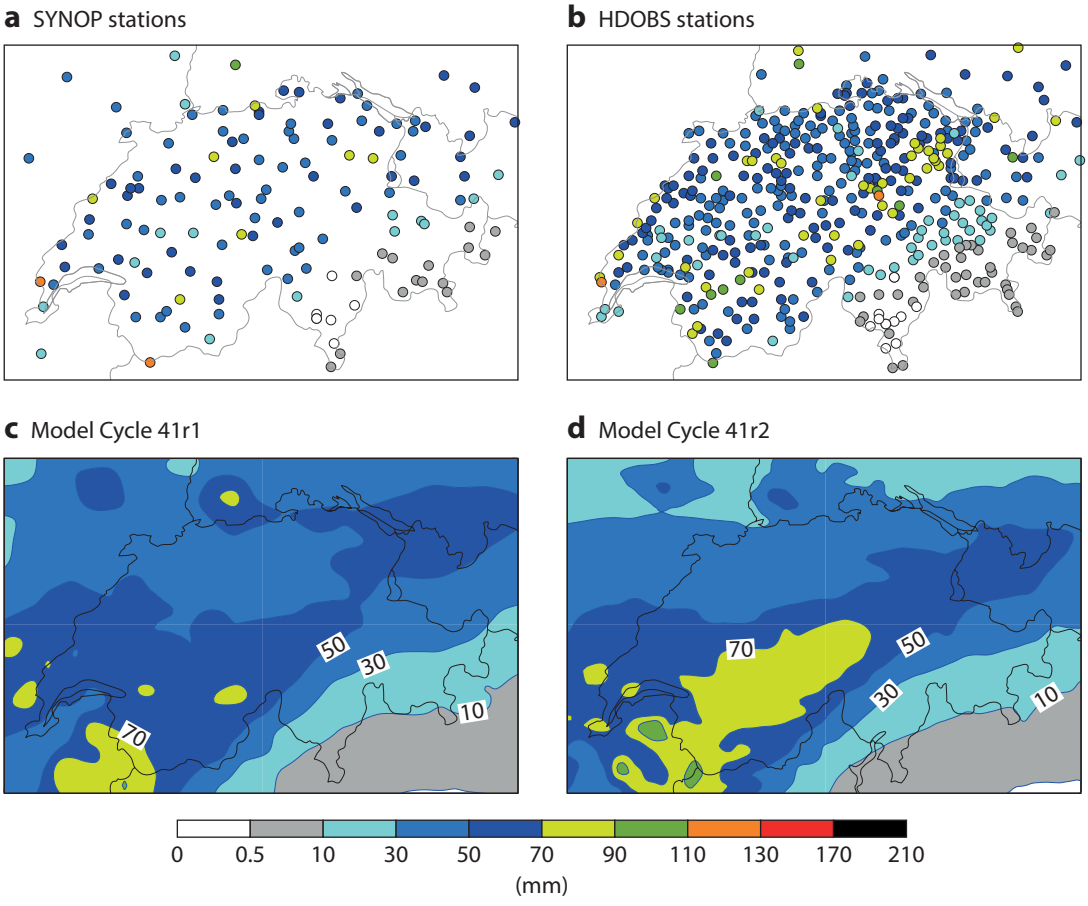

Figure 6 Observations and forecasts for a case of heavy precipitation in Switzerland, showing 24-hour precipitation totals for the period 0600 UTC on 20 November 2015 to 0600 UTC on 21 November 2015 at (a) SYNOP stations and (b) HDOBS stations, and corresponding HRES forecasts for a lead time of 3 days (54 to 78-hour forecast) from (c) model cycle 41r1 and (d) model cycle 41r2.

Figure 5 shows 48-hour totals from 0600 UTC on 1 September to 0600 UTC on 3 September 2015 as represented by SYNOP and SYNOP+HDOBS data, and corresponding HRES forecasts for a lead time of 3 days (30 to 78-hour forecast) from the then operational model cycle (41r1) and the then pre-operational model cycle (41r2). In the area shown there are 223 Norwegian HDOBS stations available compared with 118 SYNOP ones. The HDOBS stations provide a substantially better spatial representation of the most heavily affected areas, in particular the two north–south oriented bands of heavy precipitation, which are also present in the forecasts.

Switzerland – November 2015

A cold front which moved across Switzerland from the north on 20 and 21 November 2015 brought the first major snowfall of the season in the area. The snowfall line descended from 2700 m to 700 m during the course of the event, and no significant flooding was reported even though heavy precipitation was recorded in much of Switzerland outside the orographically sheltered south-east. Of the 408 Swiss HDOBS stations, 167 stations reported totals over 50 mm. One station in the Jura mountains recorded 116 mm in 24 hours. Figure 6 shows 24-hour totals from 0600 UTC on 20 November 2015 to 0600 UTC on 21 November 2015 as represented by SYNOP and HDOBS data, and corresponding HRES forecasts for forecast day 3 from the then operational model cycle (41r1) and the then pre-operational model cycle (41r2). The new model version gives a spatial distribution similar to the operational one but with larger accumulations. Although this is a large-scale event, high-density observations are important in the evaluation of forecast performance. For example, the increased precipitation in the south-western area of Switzerland in the new cycle is better supported by HDOBS than by SYNOP alone. Conversely, the HDOBS show that the underestimation of precipitation in the north-east for both cycles is more substantial than it would appear based on SYNOP only.

Evaluation of new model cycles

Apart from case studies, high-density observations also enhance the statistical evaluation which is required before a new model cycle can be put into operation. For heavy precipitation the limited time period over which the testing and comparisons extend (in the order of half a year) can make the identification of differences difficult. Higher-density observations reduce the noise in the scores and allow higher precipitation thresholds to be evaluated. Figure 7 shows a verification of the higher-resolution model cycle 41r2, implemented in March 2016, compared to the previous model cycle 41r1, for a threshold of 50 mm. The evaluation against HDOBS reduces the noise compared to SYNOP, providing a somewhat more robust indication of a positive effect of the new model cycle.

High-density observations in Australia

Up to now there has been little information about the skill of IFS precipitation forecasts in Australia. SYNOP observations available on the GTS from the region are mostly at non-standard times, and even if a shift of ±1 hour is allowed between validity time and actual observation time, there are only about 200 precipitation observations covering the whole continent. Recently, as part of ECMWF's high-density verification efforts, a set of about 1,500 stations providing 24-hour precipitation totals in near real-time has been used in routine verification. This enhanced dataset, which has been made available by the Australian Bureau of Meteorology, makes it possible to verify the tropical and subtropical parts in the north of Australia separately from the extra-tropical southern areas.

Figure 8 shows the evolution of the ETS for 24-hour precipitation at forecast day 3 for a low threshold of 1 mm, thus measuring the skill of the model in distinguishing days with precipitation from dry days. The skill averaged over the full domain has slightly increased during the period. Results for the northern and southern parts show that the increase is mainly due to improvements in extra-tropical areas.

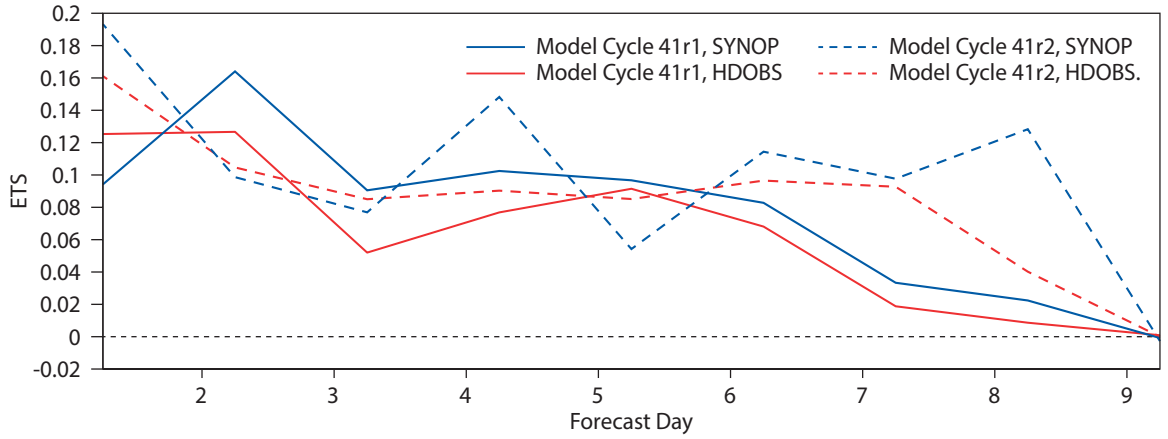

Figure 7 Equitable Threat Score (ETS) for 24-hour precipitation totals exceeding 50 mm in Turkey from model cycle 41r1 (solid lines) and from model cycle 41r2 (dashed lines) as verified against SYNOP (blue) and HDOBS (red).

As expected, scores are higher in the non-tropical part and the difference between the two sub-areas is comparable to the amplitude of seasonal variations. These variations are stronger in the tropical than in the extra-tropical areas. Station numbers in the two sub-areas are roughly comparable although the tropical part represents a larger area. This is taken into account by the density weighting which is used, and the full domain results are accordingly closer to those for the tropical area. Results for other forecast ranges and precipitation thresholds indicate overall improvements similar to those shown in Figure 8.

Summary and outlook

The collection of high-density observations from Member and Co-operating States progressed considerably in 2015 so that the dataset can now be used routinely in model evaluation. Further increases in data coverage in Europe are expected as additional countries join the initiative. In addition, ECMWF receives surface station data for Europe as part of its EFAS activities. Tests are being carried out to see how best to merge the SYNOP, HDOBS, and EFAS datasets for use in verification. Also, the use in verification of radar-based gridded precipitation datasets, such as ODYSSEY for Europe (*Lopez*, 2014a), NEXRAD for the United States (*Lopez*, 2014b), or the MERGE satellite/rain gauge combined dataset provided by the Center for Weather Forecasting and Climate Research (CPTEC, Brazil) for South America, is being investigated. Once the period covered by a dataset has reached a few years, it can be used to improve the longer-term monitoring of forecast skill.

The upscaling of precipitation observations greatly benefits from higher-density observations. This has become especially important as ECMWF explores the scale-dependence of forecast skill at different time ranges for both upper-air and surface parameters (*Buizza et al.*, 2015). In addition to gridded data based on rain gauge observations, verification against radar-based datasets is being tested for possible inclusion in routine evaluation of precipitation forecast skill (*Rodwell et al.*, 2015). Further work with high-density observations will also include evaluation of extreme wind events in areas where 10-metre wind speed HDOBS are provided. We would like to take this opportunity to thank ECMWF's Member and Co-operating States for contributing to the HDOBS effort, as well as the European Climate Assessment & Dataset (ECA&D) project for collaboration on the data transfer. Member and Co-operating States which are not yet contributing and would like to do so should contact Thomas Haiden (thomas.haiden@ecmwf.int).

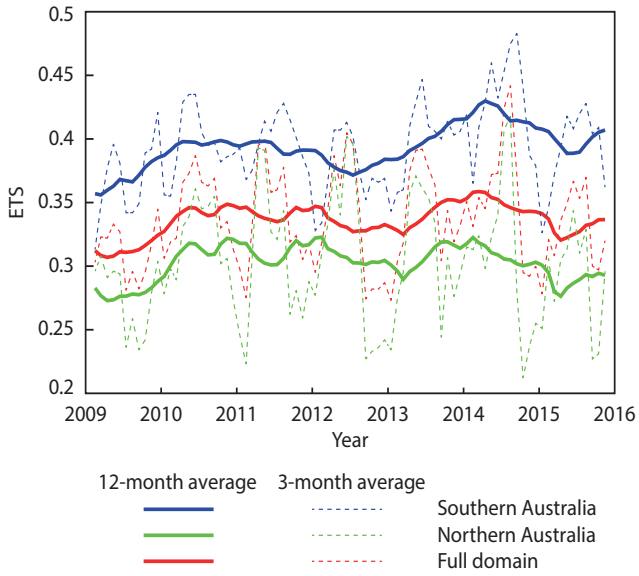

Figure 8 Equitable Threat Score (ETS) for 24-hour precipitation totals exceeding 1 mm from the HRES at forecast day 5 in Australia. Results are shown in the form of 3-month and 12-month running averages for the full domain, the northern, tropical part (<30°S) and the southern, extra-tropical part (≥30°S).

FURTHER READING

Buizza, **R.**, **M. Leutbecher** & **A. Thorpe**, 2015: Living with the butterfly effect: a seamless view of predictability. *ECMWF Newsletter* **No. 145**, 18–23.

Csima, **G.** & **A. Ghelli**, 2008: On the use of the intensity-scale verification technique to assess operational precipitation forecasts. *Meteor. Appl.*, **15**, 145–154.

Forbes, **R.**, **T. Haiden** & **L. Magnusson**, 2015: Improvements in IFS forecasts of heavy precipitation. *ECMWF Newsletter* **No. 144**, 21–26.

Göber, **M.**, **E. Zsoter** & **D. S. Richardson**, 2008: Could a perfect model ever satisfy a naive forecaster? On grid box mean versus point verification. *Meteorol. Appl.* **15**, 359–365.

Lopez, **P.**, 2014a: Comparison of ODYSSEY precipitation composites to SYNOP rain gauges and ECMWF model. *ECMWF Technical Memorandum* **No. 717**.

Lopez, **P.**, 2014b: Comparison of NCEP Stage IV precipitation composites with ECMWF model. *ECMWF Technical Memorandum* **No. 728**.

Rodwell, **M. J.**, **L. Ferranti**, **T. Haiden**, **L. Magnusson**, **J. Bidlot**, **N. Bormann**, **M. Dahoui**, **G. De Chiara**, **S. Duffy**, **R. Forbes**, **E. Hólm**, **B. Ingleby**, **M. Janousek**, **S.T.K. Lang**, **K. Mogensen**, **F. Prates**, **F. Rabier**, **D.S. Richardson**, **I. Tsonevsky**, **F. Vitart** & **M. Yamaguchi**, 2015: New developments in the diagnosis and verification of high-impact weather forecasts. *ECMWF Technical Memorandum* **No. 759**.

Diagnosing model performance in the tropics

NEDJELJKA ŽAGAR, MARTEN BLAAUW, BLAŽ JESENKO (all University of Ljubljana, Slovenia), **LINUS MAGNUSSON** (ECMWF)

Tropical circulation is an important component of weather and climate models. Tropical features of organised convection, such as the Madden–Julian Oscillation (MJO) and the El Niño–Southern Oscillation (ENSO), are believed to have a strong impact on extra-tropical circulation and are critical for extended-range predictions. Waves in tropical circulation can be excited by disturbances caused by organised convection, and these tropical waves can propagate far from their sources and spread the impact of the convection.

Error properties in forecasts of tropical circulation are more difficult to establish than in the extra-tropics, where the geopotential height often provides sufficient information about the large-scale circulation. This is a consequence of a strong coupling between the geopotential height and winds in the extra-tropics, known as quasi-geostrophic balance. In the tropics, such balance is often weak and, therefore, the flow has to be decomposed into a balanced component, which is represented by the equatorial Rossby waves, and an unbalanced component that consists of inertio-gravity (IG) waves of many scales. Such a 'modal decomposition' can provide a deeper understanding of the circulation in the tropics, and of the sources of deficiencies in analyses and forecasts.

The recently developed MODES tool provides such a decomposition into balanced (Rossby) and unbalanced (IG) modes. It has been applied to analyses and forecasts produced by ECMWF's Integrated Forecasting System (IFS) to discuss the scale-dependent energy content of Rossby and IG waves in the IFS and to analyse model performance in the tropics. Key findings include that IG modes make up a significant part of tropical circulation and are associated with significant analysis uncertainties and forecast errors.

Modelling tropical circulation

The representation of tropical circulation has significantly improved in most numerical weather prediction (NWP) systems over the last two decades (e.g. *Bechtold et al.*, 2008). However, it remains one of the biggest challenges for data assimilation in global NWP. This can be illustrated by the results of a comparison between six state-of-the-art NWP systems by *Park et al.* (2008), who showed that the root-mean-square differences between the six analyses over the tropics exceeded the climatological standard deviation of the tropical circulation. The differences among the same analyses over the extra-tropics only amounted to about 10% of the corresponding climatological variability. Significant discrepancies between NWP analyses and reanalyses in the tropics are associated with a lack of direct observations of wind profiles and with complex tropical dynamics. The latter is also a reason why multivariate data assimilation, which can successfully analyse mid-latitude weather systems by using satellite observations of radiances, is less successful in constraining tropical circulation. Mid-latitude flow is close to quasi-geostrophic balance, meaning that there is a strong coupling, at a single horizontal level, between temperature or geopotential height on the one hand and winds on the other. Such coupling is on average weak in the tropics. The most important dynamical processes in the tropics occur in relation to convection, which generates a spectrum of inertio-gravity (IG) waves.

Rossby and IG waves are obtained as eigensolutions of the linearised primitive equations and they represent balanced (primarily rotational) and unbalanced (predominantly divergent) dynamics. Similar to the role of Rossby modes in the quasi-geostrophic theory for the mid-latitudes, IG modes are important for our understanding of tropical flow features. In particular, IG waves, which are characterised by small phase speeds and are equatorially trapped, have been used to describe tropical variability on all scales in both the atmosphere and oceans. An example is the Kelvin wave, the most studied IG mode of the global atmosphere, which is believed to play a significant role in the MJO and other low-frequency features in the tropics. In spite of the large amount of research and improved understanding of the role of IG oscillations on many scales, their representation is still a source of significant uncertainties in both weather and climate models.

Analysis uncertainties in the tropics are in part associated with (a lack of) modelling of the role of large-scale equatorially trapped IG waves in data assimilation. This was demonstrated by *Žagar et al.* (2005), who showed that the apparent decoupling between the tropical mass field and the wind field in the variational assimilation is a consequence of the combination of the equatorial Rossby and IG mass-wind couplings between wind and temperature fields that have different signs. For example, the Kelvin mode is characterised by a positive coupling between the zonal wind and geopotential height at the equator. As a result, it reduces the negative coupling between the mass and the zonal wind that is imposed by the quasi-geostrophic type of balance at the equator (*Žagar et al.* 2005). This illustrates an important effect that IG modes may have in ensemble data assimilation.

Diagnosing a model's representation of divergence-dominated IG (unbalanced) circulation, and in particular of equatorial waves, can provide a better understanding of model deficiencies and new ideas for their improvement. This is the motivation behind MODES, a European Research Council-funded project at the University of Ljubljana that provides a tool for the quantification of the impact of unbalanced circulation in global NWP and climate models. The MODES software has been applied to ECMWF's analyses and high-resolution forecasts (HRES) on a daily basis since

The MODES software

A

MODES decomposes the global circulation into three-dimensional harmonic functions, more precisely into three-dimensionally orthogonal normal mode functions (NMFs) in the vertical sigma coordinate, which is naturally suited to the representation of atmospheric data. The 3D NMFs represent surface pressure, temperature and wind fields simultaneously. The method relies on a representation of the global baroclinic atmosphere in terms of *M* global shallow-water systems, each characterised by its own fluid depth for horizontal flow, known as the equivalent depth.

The projection procedure consists of a vertical projection followed by the horizontal step. The basis functions for the horizontal projection are the Hough harmonics. For every given vertical mode, the Hough harmonics are characterised by the zonal wavenumber and meridional mode. Details of the NMF representation are given in Žagar et al. (2015a), including a summary of the theory of normal-mode function expansion, instructions for the application of the MODES software, and outputs of its application to the ERA-Interim reanalysis dataset. Recently available software provides outputs also in NetCDF format.

The outputs of the modal decomposition are the complex Hough expansion coefficients, given as a function of vertical mode (*m*), meridional mode (*n*) and the zonal wavenumber (*k*). For every meridional mode, there are three solutions: a balanced mode, which obeys the dispersion relationship for Rossby waves, an eastward-propagating inertia-gravity mode and a westward-propagating inertia-gravity mode, denoted EIG and WIG, respectively.

MODES is funded by the European Research Council under the European Union's Seventh Framework Programme (FP/2007-2013)/ERC Grant Agreement no. 280153. The MODES tool and archived results are available from http://meteo.fmf.uni-lj.si/MODES. The MODES software relies on theoretical developments by Dr Akira Kasahara in the 1970s and 1980s at the National Center for Atmospheric Research in Boulder, CO, USA.

the autumn of 2014. This article presents the evaluation of large-scale tropical circulation in January and July 2015 in ECMWF forecasts. This is supplemented by a decomposition of HRES mean analysis increments in the autumn of 2015.

Decomposition of global circulation

The MODES software decomposes global dynamical fields into balanced and unbalanced (eastward- and westward-propagating IG) flow at different vertical and horizontal scales. This is achieved by representing the fields as a sum of oscillations, called Hough harmonics, with different vertical modes, meridional modes and zonal wavenumbers. The method is described in greater detail in Box A.

Since October 2014, ECMWF's operational 10-day forecast has been analysed using this method with a time step of 12 hours. The data from the 00 UTC run is analysed on 137 model levels and a reduced horizontal resolution provided by the regular Gaussian grid N128 (512×256 points in the zonal and meridional directions, respectively). However, not all vertical modes are included as the numerical solution of the vertical structure equation limits the usefulness of vertical modes with high vertical mode index. This results in an incomplete representation of the mass field in the lower troposphere (for details see *Žagar et al.*, 2015a).

Energy distribution

One of the MODES outputs is the distribution of total atmospheric energy in balanced and unbalanced components as a function of zonal wavenumber. Figure 1 shows the January 2015 average energy distribution for 00 UTC analyses and the corresponding 10-day forecasts. The energy spectra are shown up to the zonal wavenumber 180, which corresponds to a grid spacing of about 120 km at the equator and about 80 km in the mid-latitudes. As the spectral energy distribution presented in Figure 1 is different from commonly used energy spectra in the IFS, it may be useful to discuss the differences.

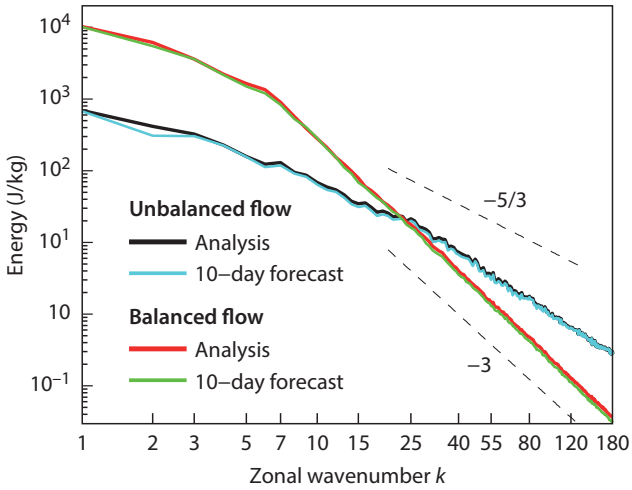

Figure 1 Atmospheric energy distribution in balanced and unbalanced flow as a function of the zonal wavenumber in January 2015 for 00 UTC analyses and 10-day forecasts. The energy is summed over all meridional and vertical scales. The zonally averaged state ($k = 0$) is not included. Short dashed lines correspond to slopes in accordance with the –3 and –5/3 laws.

The basis functions used to produce Figure 1 are the Hough harmonics, whereas global spectral models such as the IFS use spherical harmonics. The latter are the eigensolution of the global barotropic vorticity equation whereas the former are the eigensolution of the global linearised shallow-water equations. A scale-dependent distribution of atmospheric energy is readily produced from both types of harmonic representation with an important difference: the spherical harmonics provide a kinetic energy spectrum at a given horizontal level as a function of the zonal or global wavenumber, whereas the Hough harmonics provide

the spectrum of kinetic and available potential energy of horizontal motions associated with a prescribed equivalent depth (i.e. with a certain vertical mode) as a function of the zonal wavenumber and meridional mode. In other words, the spectra in Figure 1 include available potential energy and the whole model depth.

Furthermore, the application of spherical harmonics allows the decomposition of kinetic energy into rotational and divergent components, whereas the Hough harmonics provide an energy decomposition into balanced (or vorticity-dominated Rossby) and unbalanced (or IG, mainly divergent) components. The divergent energy spectra are often regarded as synonymous with IG spectra in mid-latitude mesoscale conditions. On large scales and in the tropics, such an assumption is not valid. For example, the equatorial Kelvin wave is a half-rotational and half-divergent mode and as such difficult to extract from IFS data.

Figure 1 shows that the energy spectrum for balanced flow follows the so-called 'minus 3 law' (the energy is proportional to the wavenumber k to the power of −3) all the way from the synoptic scales down to the smallest presented scale ($5 < k \leq 180$). The energy spectrum for unbalanced flow is characterised by a flatter slope than for balanced flow, especially on subsynoptic scales ($k > 15$). In this scale range, the spectrum for unbalanced flow fits the −5/3 law well, in agreement with recent studies of the role of IG motions. The energy distribution at planetary scales ($k < 5$) shown in Figure 1 is a particularly useful diagnostic produced by the MODES tool as it corresponds to the sum of kinetic and potential energy computed from the wind components and geopotential height at these scales. By contrast, the computation of rotational and divergent energy for the wavenumber k from spherical harmonics involves derivatives and thus depends on velocities in neighbouring wavenumbers.

On subsynoptic scales ($k > 15$), the energy contribution from unbalanced flow dominates. Unbalanced circulation contributes between 5% and 10% of the total wave energy depending on the forecasting model and the season (*Žagar et al.*, 2015a). For example, the planetary scales were significantly more energetic in January than in July 2015 (not shown). Figure 1 also includes the average spectra of 10-day HRES forecasts in January 2015. Comparing these with the analyses suggests that HRES tended to somewhat underpredict the variability at most scales, especially at zonal wavenumber 2.

Unbalanced circulation and Kelvin waves

The modal decomposition can be used to filter any mode and spatial scale back to physical space. For example, Figure 2 presents balanced and unbalanced flow in January and July 2015 for a level at the tropical tropopause. In January, the most significant geopotential height perturbation was present over the eastern Pacific, and it resembles the most energetic balanced mode: the Rossby wave with the lowest meridional mode (known as the $n = 1$ Rossby mode). In this region, the unbalanced winds were of the same direction, whereas over the central Pacific they were stronger and with the opposite sign compared to the balanced flow (Figure 2b,c). In July, the unbalanced winds were strongest over the Indian Ocean region in relation to the summer monsoon. Overall, Figure 2 shows that a significant component of large-scale tropical circulation is unbalanced in both months. In the lower tropical troposphere, unbalanced winds tend to be stronger than balanced winds, especially in the cross-equatorial component (not shown). On average, balanced and unbalanced flow are in opposite directions in the lower and upper troposphere near the equator, in agreement with simplified models of tropical circulation (*Žagar et al.*, 2015a).

Figure 3 shows that, on average, the equatorial Kelvin wave signal is dominated by the zonal wavenumber 1 and has the largest amplitude over the Indian ocean in July. The propagation of Kelvin waves in the model forecasts is illustrated in Figure 4. Here, we put together results of the modal decomposition every 12 hours and show both zonal wind and temperature perturbations, computed from geopotential perturbations using the hydrostatic relationship. Although the decomposition is performed independently for each time step, when the outputs for successive times are put together, they naturally connect and show propagation properties known from linear theory and studies based on frequency filtering. This is a strong justification for the assumptions made for the derivation of normal modes used for the decomposition. Figure 4 shows how wind and temperature perturbations associated with the zonal wavenumber 1 Kelvin wave propagate in the equatorial stratosphere at a speed of around 60 m/s. It should be noted that the presented wave properties are the result of a summation over 70 vertical modes. The maximum energy in this case is found around vertical mode 8, which corresponds to an equivalent depth of around 450 metres, implying a shallow-water phase speed of around 65 m/s.

Evaluation of tropical forecast errors

Similar to the way in which the amplitudes of spherical harmonics can be compared, a scale-dependent evaluation of atmospheric circulation can be carried out by using the Hough harmonics to compare forecasts and verifying analyses at each spatial scale (*Žagar et al.*, 2015b). The verification can also be performed in physical space for any mode of interest. This is shown in Figure 5, which presents the root-mean-square errors (RMSEs) of forecasts compared to analyses (00 UTC) for the balanced and unbalanced zonal wind component at a model level close to 50 hPa, averaged between 5°N–5°S.

The growth of RMSEs in Figure 5 is associated with the variability of the tropical stratosphere, which is driven by vertically propagating equatorial waves associated with convection. In July, convection is most intense over the maritime continent and the errors in stratospheric circulation first develop here. The RMSEs for the balanced zonal wind appear to propagate westward (Figure 5a). By contrast, the RMSEs of the stratospheric unbalanced zonal wind component propagate eastward in forecasts in both July (Figure 5b) and January (not shown), but the error amplitudes are greater and develop earlier in the forecasts

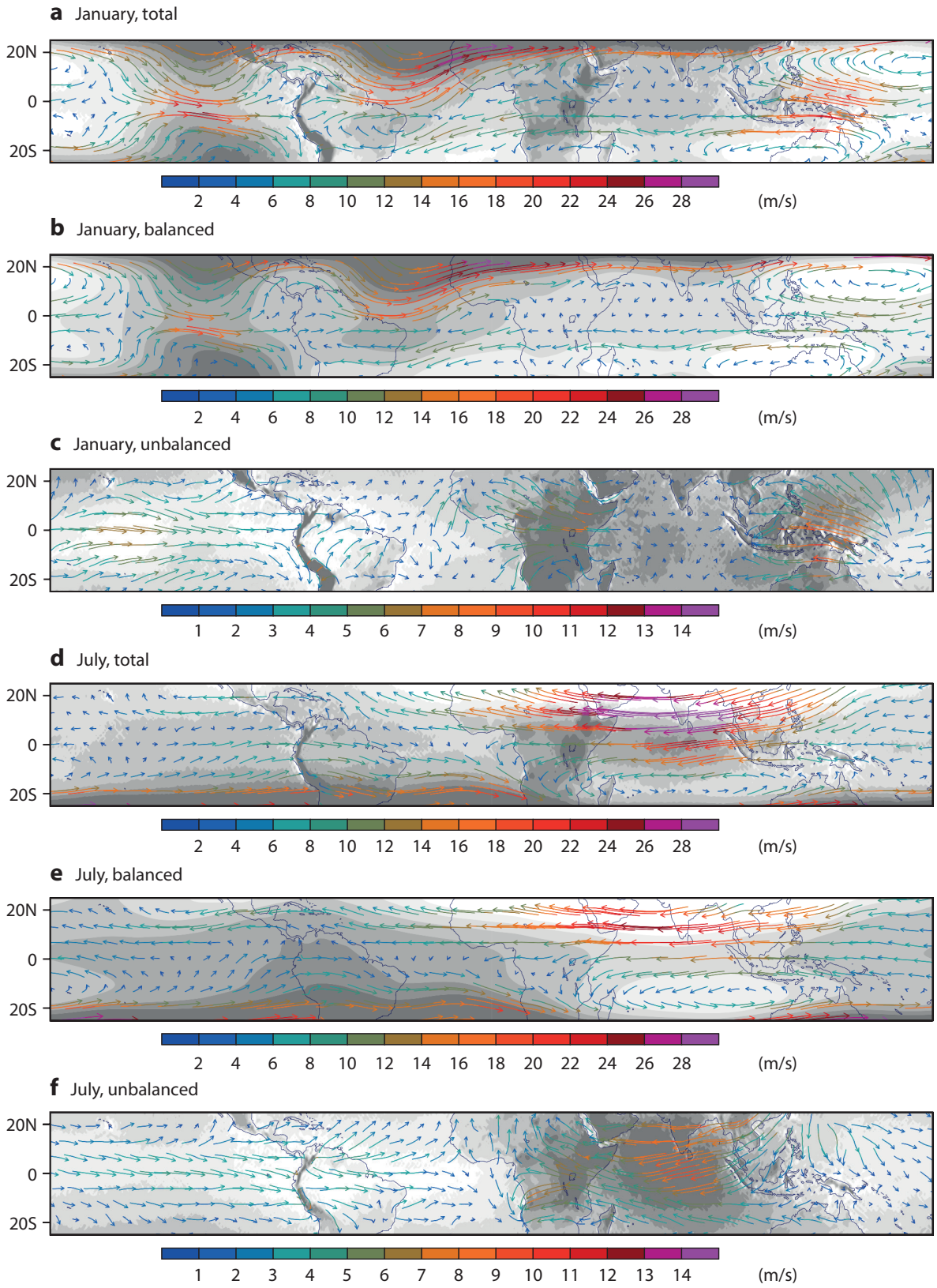

Figure 2 Average horizontal winds and geopotential height (shading) at model level 60 (approximately 100 hPa) in the tropics in January 2015 showing (a) total average flow, (b) balanced average flow and (c) unbalanced average flow; and in July 2015 showing (d) total average flow, (e) balanced average flow and (f) unbalanced average flow. Averaging is performed for analyses at 00 UTC. Note that here the presented levels are sigma levels and geopotential height is a modified geopotential variable that includes surface pressure. As a result, circulation follows the terrain throughout the model depth. Geopotential height is visualised by five contours between the maximal and minimal value in each panel.

in July. The location of the maximal stratospheric RMSE is not the same in January and July as the most intense convection, which generates vertically propagating IG waves, moves along the equator (not shown).

The fact that RMSEs for balanced flow along the equator in Figure 5a,b appear smoother than RMSEs for unbalanced flow can possibly be explained by the dynamical properties of IG waves and their generation by physical processes. At the same time, these processes may still be somewhat underrepresented in the forecasts, as suggested by Figure 1 and by looking at the growth of the ensemble spread in operational ensemble forecasts (*Žagar et al.*, 2015b).

The growth of zonally averaged tropical forecast errors in the zonal wind component is largest in the balanced component in the upper troposphere. In the 10-day range, the balanced error at level 150 hPa is nearly twice as large as the error in the unbalanced component (Figure 5c,d). The two components initially have similar amplitudes, which indicates that the analysis errors relative to the variability of the wind is higher in the unbalanced component compared to the balanced component, or possibly that the error growth is much higher during the first forecast day. In the stratosphere (level 50) the unbalanced component of error dominates in both January and July but the error growth is greatest in July, when convection is stronger. In the next section we are going to discuss short-range errors by presenting average analysis increments.

Decomposition of analysis increments

Another useful error decomposition is presented in Figure 6, which shows zonal wind analysis increments in autumn 2015 as the mean absolute differences between the analysis and the first-guess forecast. The average increments are small if the short-range forecast (first-guess) agrees with the available observations. The increments are also small if there was no significant error growth in the short-range forecast. In general, one expects the increments to be larger in dynamically active regions with faster

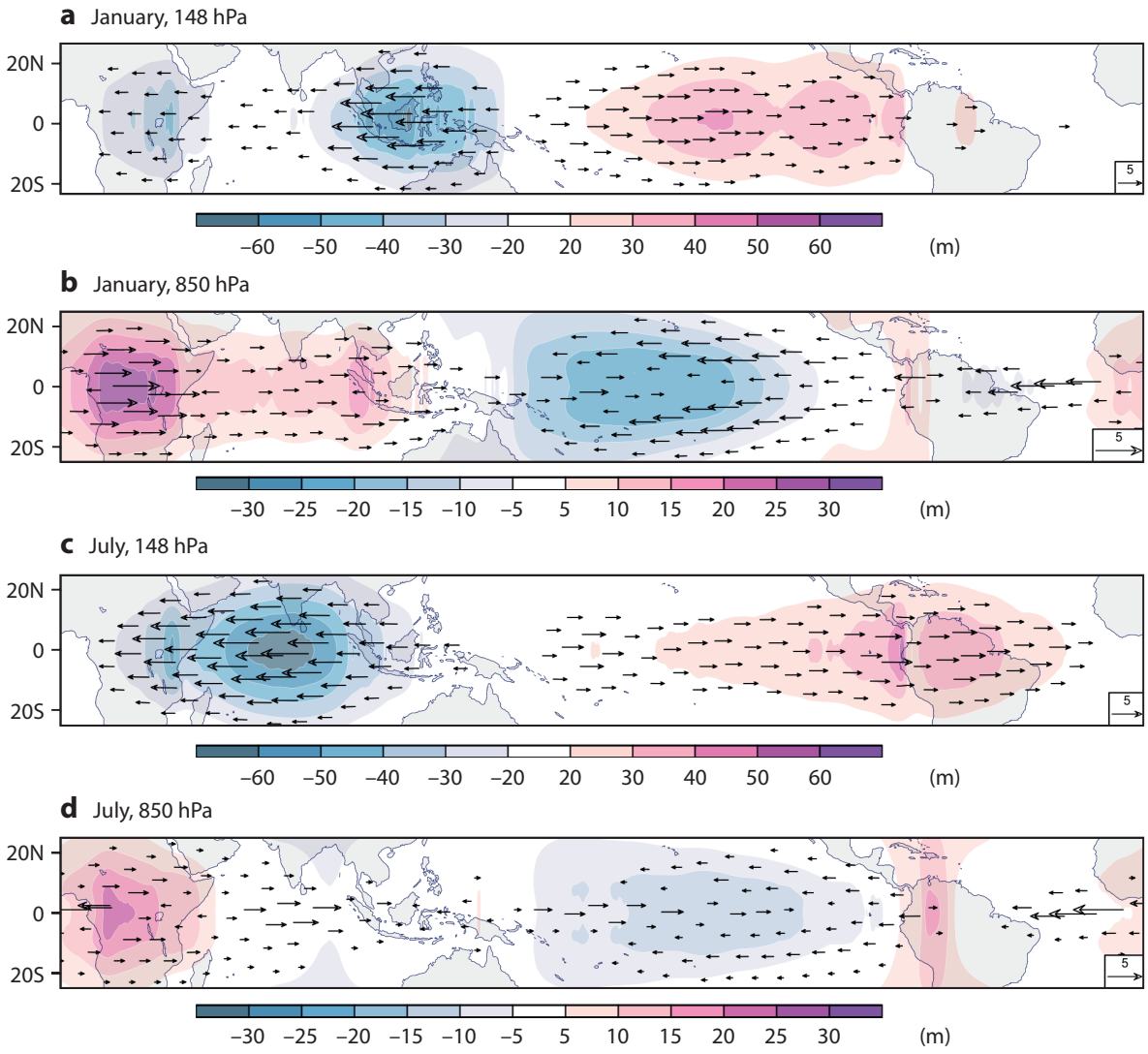

Figure 3 Kelvin wave winds (arrows) and geopotential height perturbations (shading) in January 2015 at (a) model level 68 (approx. 148 hPa) and (b) level 114 (approx. 850 hPa); and in July 2015 at (c) level 68 and (d) level 114. Averaging is performed for analyses from 00 UTC.

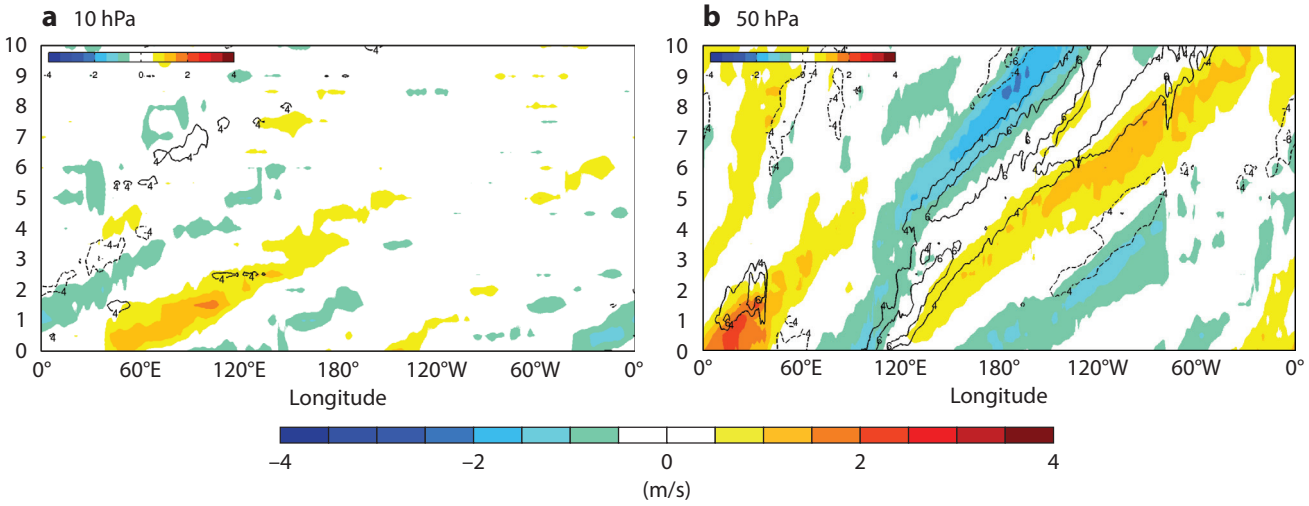

Figure 4 The evolution of Kelvin waves in the 10-day forecast started on 20 July 2015, 00 UTC, showing zonal wind speed perturbations (shading) and Kelvin wave temperature perturbations (isolines every 2 K), with positive perturbations drawn in solid lines and negative perturbations in dashed lines, for (a) level 29 (approx. 10 hPa) and (b) level 48 (approx. 50 hPa).

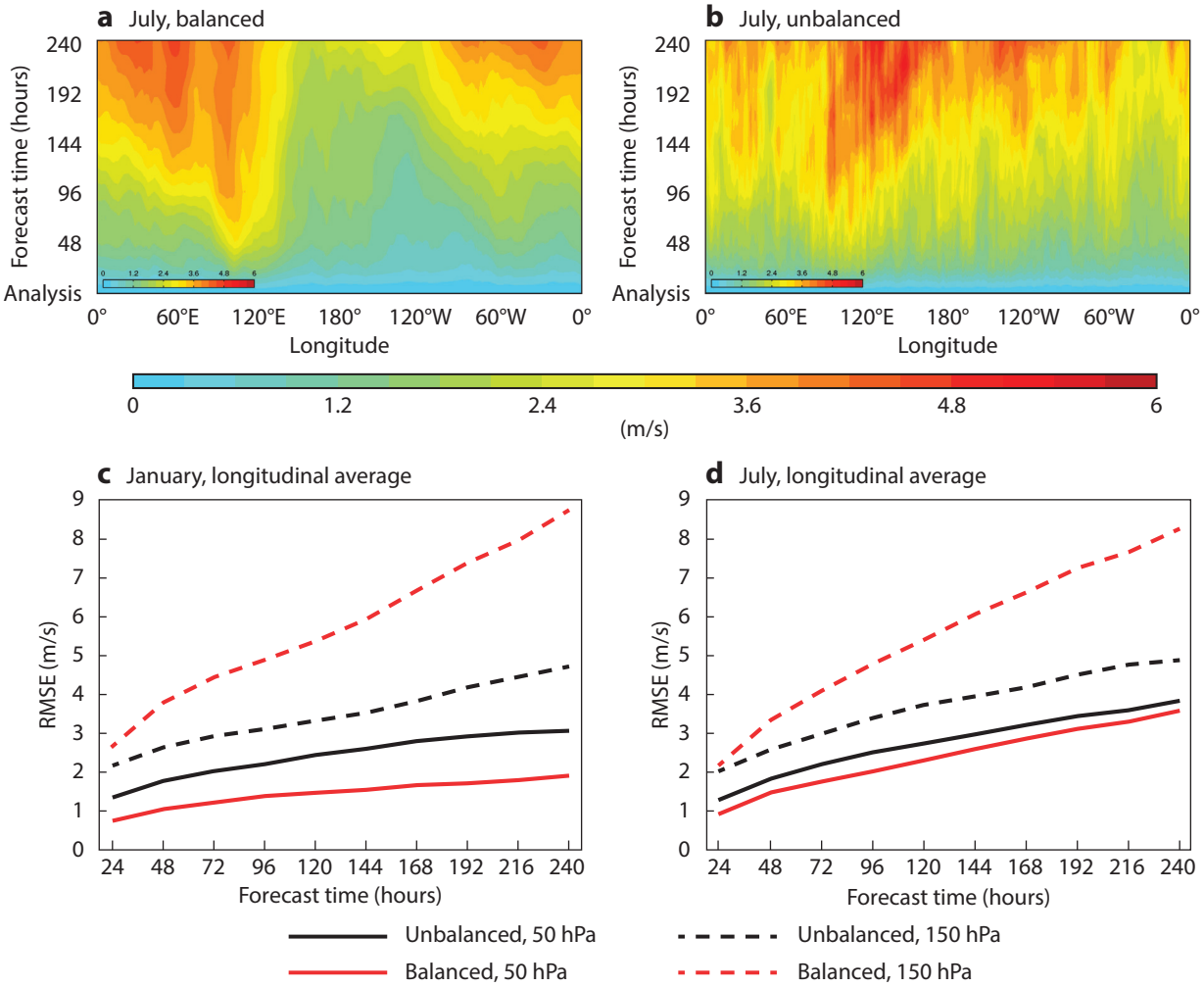

Figure 5 Root-mean-square error (RMSE) of forecasts compared to verifying analyses of tropical zonal winds, averaged over the ±5° belt around the equator, for (a) balanced winds in July 2015 at level 48 (approx. 50 hPa) and (b) unbalanced winds in July 2015 at level 48; and averaged longitudinally at level 48 and level 68 (approx. 150 hPa) for (c) January 2015 and (d) July 2015.

intrinsic error growth (e.g. in the presence of convection or baroclinic instability) and in regions with large model uncertainties (error). To understand the nature of errors, the decomposition of the increments into balanced and unbalanced components could be valuable.

Global analysis increments for all modes, split into balanced and unbalanced modes, are shown in Figure 6 at two model levels. The level close to 150 hPa represents the flow in the upper troposphere in the tropics and in the lower stratosphere in the mid-latitudes. The increments are largest at the 150 hPa level in the tropics. As discussed in *Žagar et al.* (2015b), this is the region with the largest initial-state uncertainties and the largest initial growth of the spread in ensemble forecasts. Lower in the troposphere, the increments are distributed more evenly and appear smoother, especially for the balanced component in the mid-latitudes. Note also that smaller increments at the 150 hPa level in the extra-tropics are above the tropopause, where variability is significantly smaller.

In the tropics, a larger part of increments is associated with unbalanced modes than with balanced modes at both levels. The largest increments are found over tropical Africa. A further diagnostic into various modes reveals that some of the increments over Africa are associated with the Kelvin modes (not shown). Furthermore, these increments, which are believed to be connected to convection over Africa, are strongest during daytime (18 UTC analysis). There are also big increments in unbalanced flow over eastern Africa, which is related to very localised (and unrealistic) convection in the model over Ethiopia. This feature has been improved in the new IFS model cycle (41r2). Overall, Figure 6 suggests that data

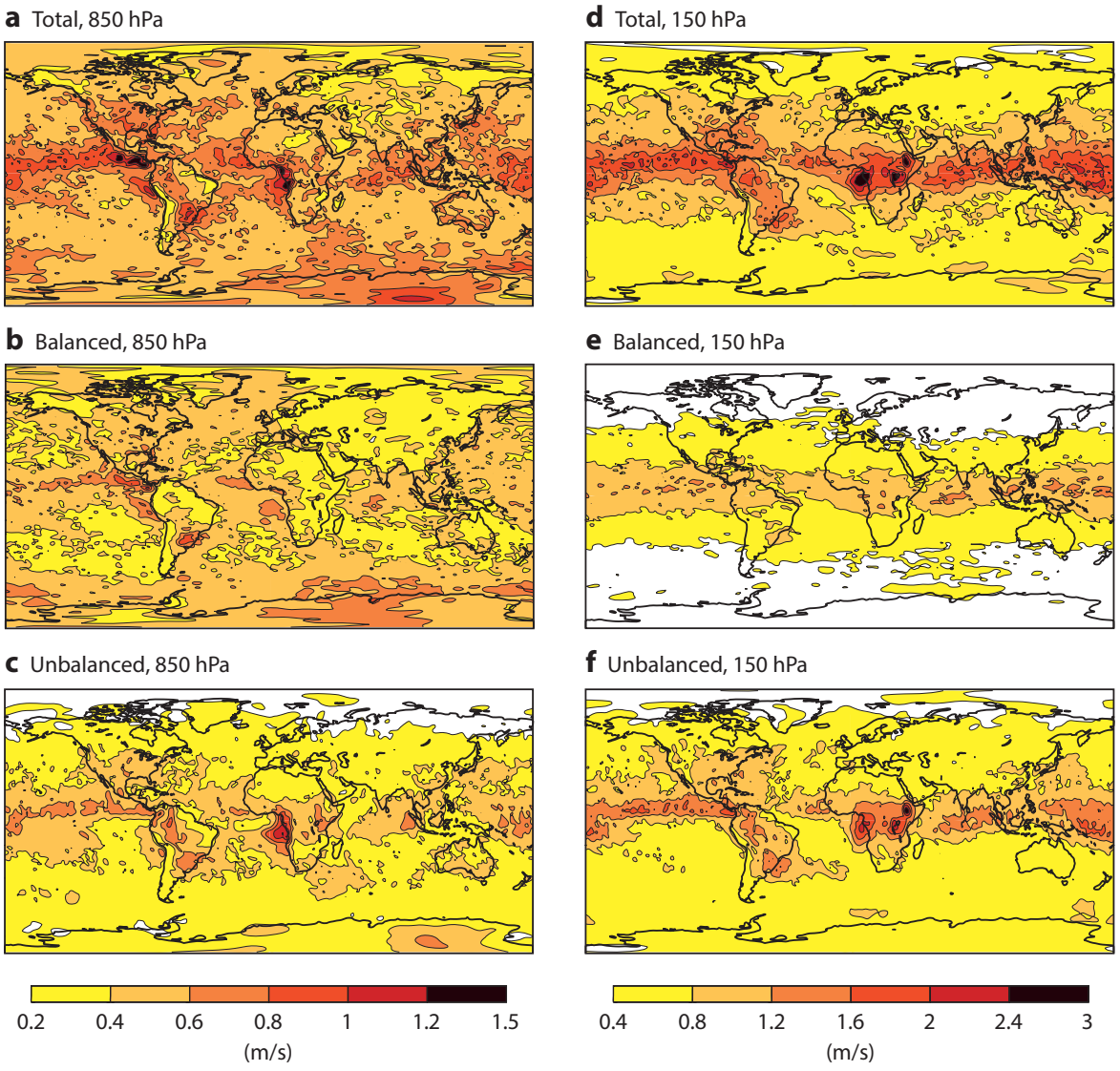

Figure 6 Mean analysis increments of zonal wind from September to November 2016 showing (a) total increments at model level 114 (approx. 850 hPa), (b) balanced increments at level 114, (c) unbalanced increments at level 114, (d) total increments at level 68 (approx. 150 hPa), (e) balanced increments at level 68, and (f) unbalanced increments at level 68. Increments are computed as mean absolute differences between 12-hour forecasts and analyses valid at 18 UTC.

assimilation is most difficult in the tropics, where forecast errors grow fastest and where a lack of direct wind observations makes it difficult to constrain circulation in the analyses. Figure 6 also shows that in high-resolution forecasts a significant part of tropospheric analysis increments projects onto unbalanced modes in the extra-tropics too.

Conclusions and outlook

We have presented a new diagnostic technique that can usefully be applied to ECMWF forecasts in the tropics and that complements other methods to validate model performance. Based on a decomposition into balanced and unbalanced (IG) modes, the technique enables balanced flow features, such as individual equatorial Rossby waves, and unbalanced waves, such as Kelvin waves, to be evaluated separately. In this way, we can more easily relate errors in forecasts to initial-state uncertainties and model errors.

We have only given a few examples of how the modal technique can be applied. Combined with similar diagnostics of data assimilation and forecast model performance in the tropics, the results suggest that there is a need for more advanced data assimilation to better constrain large-scale equatorially trapped waves in the analysis. Although the presented upper-troposphere tropical forecast errors grow more rapidly in the balanced modes, the analysis increments at the same levels are larger in unbalanced modes than in balanced modes, suggesting shortcomings in the analysis of unbalanced structures. We focused on large scales where the tropical analysis uncertainties are relatively large and where the ensemble data assimilation could benefit from the use of flow-dependent background-error covariances associated with equatorial wave dynamics.

FURTHER READING

Bechtold, **P.M.**, **M. Koehler**, **T. Jung**, **F. Doblas-Reyes**, **M. Leutbecher**, **M.J. Rodwell**, **F. Vitart** & **G. Balsamo**, 2008: Advances in simulating atmospheric variability with the ECMWF model: from synoptic to decadal time-scales, *Q. J. R. Meteorol. Soc.*, **134**, 1337–1351.

Park, **Y.-Y.**, **R. Buizza** & **M. Leutbecher**, 2008: TIGGE: preliminary results on comparing and combining ensembles. *Q. J. R. Meteorol. Soc.*, **134**, 2029–2050.

Žagar, **N.**, **E. Andersson** & **M. Fisher**, 2005: Balanced tropical data assimilation based on study of equatorial waves in ECMWF short-range forecast errors. *Q. J. R. Meteorol. Soc.*, **131**, 987–1011.

Žagar, **N.**, **A. Kasahara**, **K. Terasaki**, **J. Tribbia** & **H. Tanaka**, 2015a: Normal-mode function representation of global 3D datasets: open-access software for the atmospheric research community. *Geosci. Model Dev.*, **8**, 1169–1195.

Žagar, **N.**, **R. Buizza** & **J. Tribbia**, 2015b: A three-dimensional multivariate modal analysis of atmospheric predictability with application to the ECMWF ensemble. *J. Atmos. Sci.*, **72**, 4423–4444.

NWP-driven fire danger forecasting for Copernicus

FRANCESCA DI GIUSEPPE, FLORIAN PAPPENBERGER, FREDRIK WETTERHALL, BLAZEJ KRZEMINSKI (all ECMWF), JESÚS SAN-MIGUEL-AYANZ, ANDREA CAMIA, GIORGIO LIBERTÀ (all Joint Research Centre in Ispra, Italy)

A system to monitor and forecast wildfire danger in Europe is currently being developed in the framework of the EU-funded Copernicus Emergency Management Service. It aims to provide timely information to civil protection authorities in 39 nations across Europe by flagging up regions which might experience fire events due to high fire danger conditions. A novelty of the European Forest Fire Information System (EFFIS) is that it relies exclusively on weather forecasts to provide atmospheric forcings. This makes it possible to produce global fire danger forecasts with extended lead times. The traditional approach is for operational fire danger forecasting systems to be driven by local observations, mostly from weather observation stations.

ECMWF has developed EFFIS's global fire danger modelling component, the Global ECMWF Fire Forecasting model (GEFF), over the last three years through a third-party agreement with the European Commission's Joint Research Centre (JRC). GEFF is also the fire danger engine of the Global Wildfire Information System (GWIS), which is a GEO (Group on Earth Observations) initiative. GEFF uses the Centre's medium-range and extended-range ensemble forecasts to drive three fire danger models originally developed in the 1970s by the US, Canadian and Australian forest services. Global EFFIS fire danger forecasts are available in a GWIS beta viewer on the JRC Forest website (Figure 1).

Tests show that fire danger indices calculated by GEFF from numerical weather prediction (NWP) outputs are in principle able to identify and predict high-danger conditions for fire events in large parts of the globe. The EFFIS products are therefore useful for both disaster management and planning preventive actions to confine fire-related damage. However, the system's predictive capabilities are geographically uneven. Where vegetation fuel availability is large, such as in boreal forests, the Mediterranean, South America and Central Africa, fire events are mainly the result of drought conditions and predictability is high. On the other hand, in temperate regions where vegetation fuel availability is limited, such as the mountainous regions of Central Europe, outbreaks of fire can depend on highly variable conditions, such as the

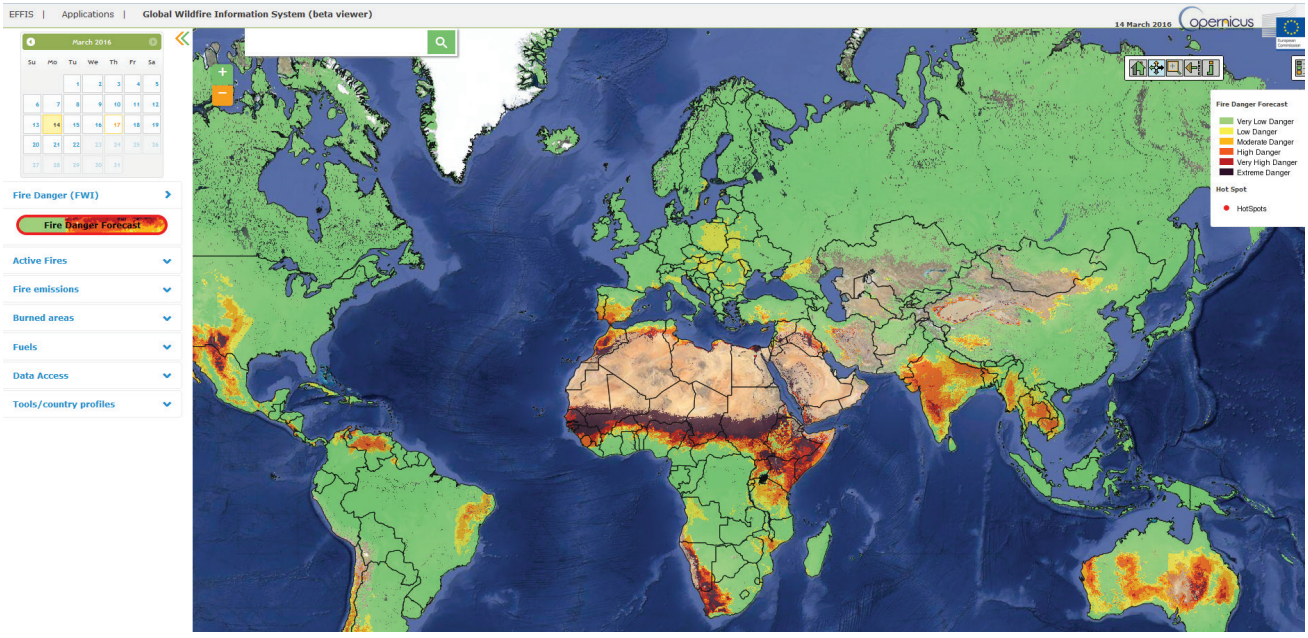

Figure 1 Screenshot of the Global Wildfire Information System (GWIS) beta viewer available via the JRC's EFFIS web page, showing a three-day global fire danger forecast for 17 March 2016. The fire danger classes are based on the output of the Canadian model and have been calibrated for Europe. The calibration of the fire danger classes outside Europe is the subject of ongoing development work.

Fire danger forecast

Very low danger | Moderate danger | Very high danger

Low danger | High danger | Extreme danger

Hotspot

short-term superficial drying of the available organic matter on the ground. In these ecosystems the system's predictive power tends to be lower.

Fire danger modelling

Fire danger is intended as a general term to express an assessment of both fixed and variable factors of the fire environment that determine the ease of ignition, rate of spread, difficulty of control, and fire impact. Fire danger therefore has several components and it is quantified using a combined metric expressing the probability of ignition, the speed and likelihood of spread and the availability of fuel. A model of fire danger is inherently probabilistic since it provides values related to the probability that a cause of ignition will result in a major outbreak. This means that extreme fire danger might or might not be followed by real fires, depending on whether or not there is a natural or human trigger. To establish whether fire danger conditions are in place, a fire danger model describes the effects that short-term and long-term variations in atmospheric temperature, humidity, precipitation and wind have on fuel moisture content and consequently on fire behaviour and occurrence. The US National Fire Danger Rating System (NFDRS), the Canadian forest service Fire Weather Index (FWI) and the Australian McArthur (MARK-5) model are all based on these concepts. They are routinely employed in those countries by forest management agencies to support fire control and suppression measures.

Traditionally fire danger evaluation has not benefited from modelling based on global weather predictions. Instead, danger conditions in forest centres are calculated using data from weather observation stations, where an evaluation of the vegetation state is also recorded. The resulting fire danger rating is then extrapolated to a large but undefined area surrounding the observation site. Thus, the real novelty of GEFF is that it implements a pure modelling approach based on ECMWF's weather forecasts. Although locally this approach may result in a loss of accuracy due to the use of more approximate forcings, it has the advantage that it can provide global forecasts with an extended lead time.

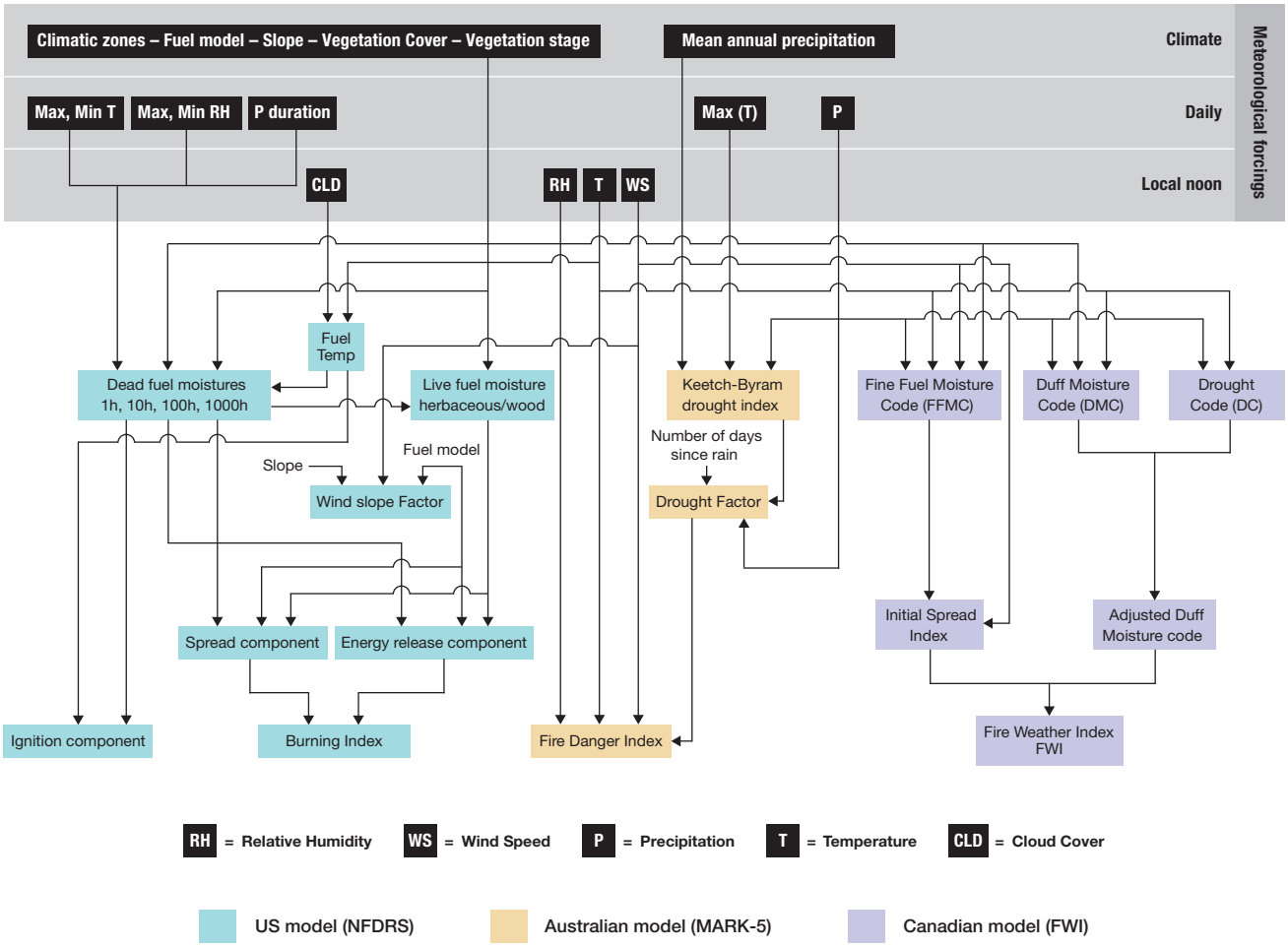

Figure 2 Schematic representation of GEFF model components with input and output connections. Three fire danger rating systems (FWI, NFDRS and MARK-5) are implemented using the same atmospheric forcings. Input data are grouped in three tiers. Tier 1 data are climatological fields which are pre-computed and kept invariant during the runs. They include vegetation type, fuel model and orography. Tier 2 data are daily values such as daily precipitation, and minimum and maximum temperature. Tier 3 data represent instantaneous values at 1200 local time.

GEFF

GEFF is a multi-model platform in which all three available rating systems are implemented (Figure 2). Each of the three fire rating systems incorporated into the GEFF model provides a comprehensive set of outputs which characterise different aspects of fire danger conditions. The indices put out by the three models in GEFF are not directly comparable. For the same kind of fire danger conditions, the GEFF values of the Fire Weather Index (FWI) from the Canadian model, the Fire Danger Index (FDI) from the Australian model and the Ignition Component (IC) from the US model can be very different.

The reason for this is that the different models apply different responses of the vegetation to weather forcings. For example, the FWI system is specifically calibrated to describe the fire behaviour in a standard jack pine stand (*Pinus banksiana*) typical of Canadian forests. The NFDRS model, on the other hand, implements a full description of vegetation through fuel type characterization and explicitly calculates the moisture content of dead and living vegetation. It divides dead fuel into classes according to their fast or slow response to changes in atmospheric temperature and humidity forcing, while living fuel is divided into herbaceous and woody and shrubs. Contrary to the other two models, the MARK-5 model includes no explicit description of the evolution of moisture in different fuel types. Instead, danger conditions are simply evaluated on the basis of a generic drought index representing fuel availability, called the Drought Factor (DF).

These differences make a direct comparison difficult and represent a barrier to integrating the different indices in an early warning application. The problem can be addressed by performing an index calibration based on historical index values: for any given location, any index value I is replaced by the relative frequency of historical occurrence of index values $\leq I$. This relative frequency is measured by the cumulative distribution function, as illustrated in Figure 3. The normalised index thus takes values between zero and one. The calibration is usually performed in terms of quartiles and the information is summarised in danger classes, so that for example when the normalised index is above the second quartile, the danger is considered high.

In the following we limit the analysis of fire predictability in GEFF to the FWI, in the interest of providing a concise analysis of generic fire danger predictability. In the actual operational implementation of EFFIS, once high-risk areas have been identified, a more detailed analysis can be performed to characterise the event in terms of, for example, expected fire containment actions required. In operational practice this is usually achieved by also gathering information provided by all the other indices calculated in GEFF (Ignition component, Burning Index, and Fire Danger Index – see Figure 2).

Potential predictability

The skill of GEFF in predicting fire danger and behaviour ultimately depends on two factors:

- the accuracy of the modelling components which translate the status of the vegetation into fire danger
- the accuracy of the predictions of atmospheric conditions driving the model.

Model accuracy defines the upper boundary of the achievable skill of such a system. This is often called potential predictability and can be estimated by reducing errors in the forcings. This can, for example, be achieved by using atmospheric reanalysis. These datasets are created by combining a single, consistent model with quality-controlled observations of past conditions in an optimal way by means of a data assimilation scheme. A reanalysis provides a dynamically consistent estimate of the climate state at each time step and can be used as a good proxy for observed meteorological conditions. Being a model integration, it has the added benefit of providing a set of global fields, including variables which are not generally observed. How close reanalysis outputs are to actual meteorological conditions depends on the number and quality of observations available and on the accuracy of the model and of the assimilation scheme used. Even with these caveats in mind, fire danger indices calculated from reanalysis datasets are less affected by uncertainties in atmospheric forcings when compared to indices calculated from forecast fields. Therefore reanalysis fire indices can be compared to observed occurrences of fire to understand the potential predictability of fire danger provided by the modelling components, and to highlight the limitations of those components.

Fire index reanalysis has been performed using atmospheric forcings from ERA-Interim. The original data resolution of around 80 km was interpolated to a lat-lon regular grid of 0.25° to be comparable with the available observational dataset of fire events (Box A). Figure 2 shows which input data are needed to run GEFF and how the atmospheric forcings are linked to the various output components of each fire index system. The reanalysis dataset for fire

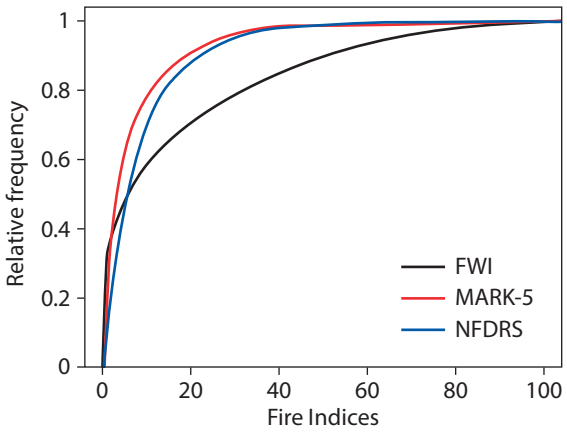

Figure 3 Cumulative distribution functions for the three indices. For any value X > 0 of a given index, the CDF represents the relative frequency of cases for which the index was greater than zero and smaller than or equal to X. For example FWI > 40 occurs in only about 20 % of cases.

danger was calculated starting from 1 January 1979 and running for 36 years with a daily time step, in accordance with the availability of ERA-Interim data. Since the initial conditions for vegetation are set using an idealised state, the fire variables suffer from the so-called 'spin up' in the first few months of the forecasts as the model drifts to its equilibrium state. The first year of simulation was therefore discarded from further analysis. For this reanalysis run, all the fire indices were set to zero if snow was on the ground or the daily precipitation was above 1.5 mm/day. Areas where vegetation fuel is not available were masked out.

Regional variations

A regional analysis is necessary to understand in which countries/regions EFFIS and its model component GEFF provides sufficient potential predictability to be useful to plan fire control actions. The regional analysis is performed using the Extremal Dependence Index, a metric which is suitable for rare events (Box B). For any grid area a predicted fire is defined when the FWI value for that day is greater than the second quartile of its time series distribution available for the 35 years of reanalysis runs. An observed event is defined if at least 10% of the grid area (i.e. 2,500 hectares) has been burned as recorded by the GFED4 dataset (see Box A).

Figure 4 shows that potential predictability is very good in regions of the globe covered by boreal forests (taiga ecosystems). Since the boreal forest zone consists of a mixture of conifers (white and black spruce, jack pine, tamarack, and balsam fir), it is not surprising that the FWI performs very well, being specifically calibrated for this vegetation cover. Potential predictability is higher in the Canadian Boreal Shield West ecozone, where large fires occur frequently, than in Canada's Montane Cordillera ecozone, where fires are numerous but tend to be smaller. The northern boreal parts of Eurasia and Siberia present a range of fire weather conditions very similar to those in boreal Canada. In these regions the vegetation is quite homogeneous and the values of the indices are controlled

Observed fire

A

National inventories of wildfire events exist in many countries, but they do not provide the global coverage and/or the extended record needed for the validation of a fire danger system at a global scale. Satellite observations can supply a valid alternative, especially as they cover remote areas where in-situ observations are sparse. Satellite data have been used to monitor biomass burning at regional and global scales for more than two decades, using algorithms that detect radiative emissions from active fires at the time of satellite overpass, and in the last decade by using burnt-area algorithms that directly map the spatial extent of the area affected by fires.

The burnt-area dataset of the Global Fire Emissions Database (GFED4) combines several satellite products in a homogeneous time sequence of events from August 2000 to the present. It provides daily burnt-area fraction data with a 0.25° resolution. GFED4 combines 500 m MODIS satellite burnt-area maps with active fire data from the Tropical Rainfall Measuring Mission (TRMM) Visible and Infrared Scanner (VIRS) and the Along-Track Scanning Radiometer (ATSR) family of sensors. The daily burnt-area dataset is used in this article to validate the relationship between the modelled fire danger and the observed occurrence of fire episodes.

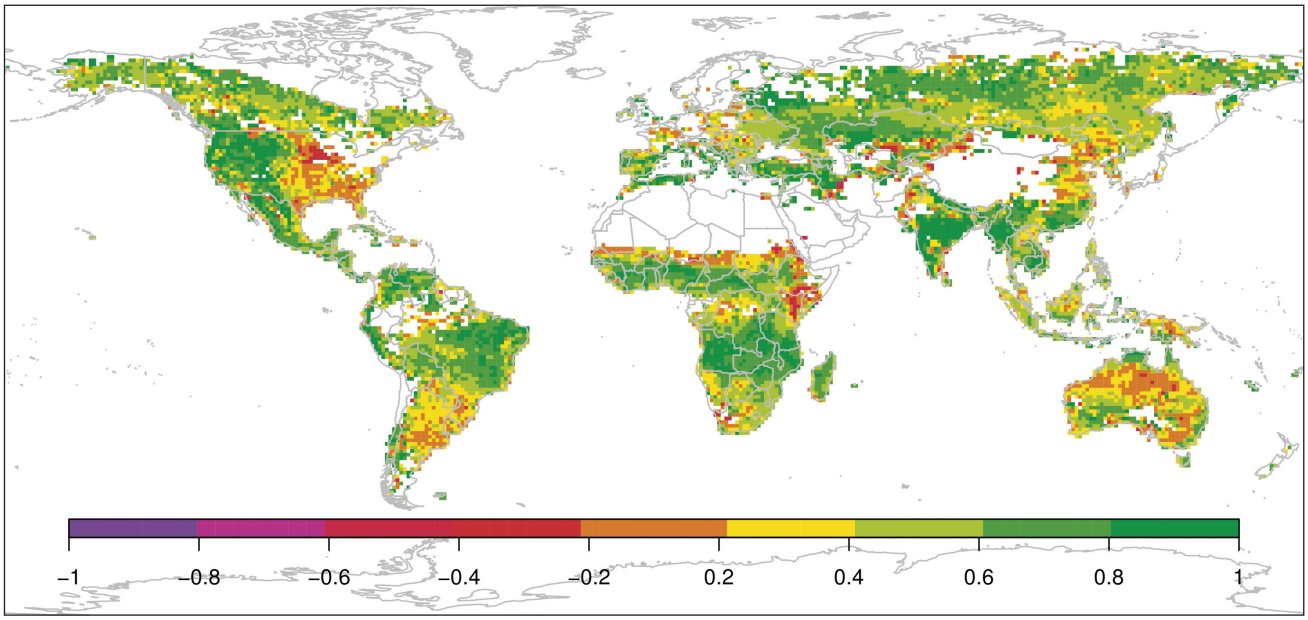

Figure 4 Extremal Dependence Index (EDI) for the Fire Weather Index (FWI). The EDI skill score is calculated using the fire mask derived from the GFED4 dataset. A fire is considered to have been forecast when the FWI is above the second quartile (> 50%) of its distribution. EDI takes the value of 1 for perfect forecasts and 0 for random forecasts. Therefore the system beats a random forecast if its EDI score is above zero, in which case it can be considered to have some skill.

Assessing fire danger predictability

B

		Event observed: Yes	Event observed: No
Event forecast	Yes	A Hits	B False alarms
	No	C Misses	D Correct negatives

Assessments of potential fire danger predictability have to take into account that fire events are rare. Assessing the quality of predictions is therefore complicated by the fact that measures of forecast quality typically degenerate to trivial values as the rarity of the predicted event increases. This can be seen by considering a contingency table for observed and predicted fire events. Once the occurrence of an event has been defined for the forecast (for example if and only if FWI > 3rd quartile), it is possible to count the number of hits (A), misses (B), false alarms (C) and correct negatives (D) by comparing forecasts with observations. The resulting table can be used to derive skill measures. It can be shown that common skill scores tend to vanish as the base rate of observed events $\frac{A+C}{A+B+C+D} \Rightarrow 0$, regardless of actual forecast skill.

The Extremal Dependence Index (EDI) has been shown to be less dependent on the base rate and can be used to assess the potential predictability of fire danger. EDI provides a skill score in the range [-1, 1]. It is a function of how fast the hit rate converges to zero as the event becomes more rare, as opposed to being based on the base rate. EDI takes the value of 1 for perfect forecasts and 0 for random forecasts. It is greater than zero for forecasts that have hit rates that converge to zero more slowly than those of random forecasts and can be negative in the opposite situation. Therefore a system beats random forecasts if its EDI score is above zero, in which case it can be considered to have some skill.

mostly by weather forcings. Despite the similarity in vegetation type, fire regimes can be very different, with fires in Siberia tending to be smaller than in Canada and relatively frequent, and to have moderate to high intensity. Unfortunately the observation dataset spans only 13 years, which means that areas such as the Nordic countries have too few events for a reliable assessment of potential predictability.

In Australia fires can develop in two very different environments. They can either burn in mountainous areas, which are usually densely forested, or they can start on plains or areas of small undulation predominantly made up of grassland or scrubland. In the first case fire episodes can be extremely intense and long-lived, while in the second case fires move quickly, fuelled by high winds in flat topography, and quickly consume the small amounts of fuel/vegetation available. Potential predictability using GEFF is reasonably good in either of these two regimes, but GEFF performs better in forested areas.

Wildfires in Southeast Asia, including in Thailand, Malaysia and Indonesia, tend to be human-caused. It is a common practice in Indonesia to start fires during the dry season (July to October) to clear land and remove agricultural residues. During intense dry seasons, these fires can penetrate into degraded sub-surface peat soil with enhanced flammability. Since such fires only tend to die down with the arrival of the heavy precipitation associated with the onset of the monsoon, fire seasons in these regions are controlled by rainfall seasonality associated with monsoon activities, which produce an annual or, in some regions, semi-annual wet–dry cycle. Although these ecosystems are very different from boreal forests, the FWI index performs reasonably well as an indicator of fire danger. This is not surprising since the occurrence of fires heavily depends on the prevalence of dry conditions, which are well represented in the reanalysis dataset used.

In the Mediterranean, vegetation is dominated by a combination of shrubland and low forests. Persistent dry climatic conditions in summer favour the establishment of intense fire seasons in areas where fuel is available. Again, despite the very different type of vegetation compared to boreal forests, the FWI performs remarkably well in identifying fire danger in these ecosystems, especially in the southern parts of Spain, Greece and Italy.

The climate in central Europe is sub-continental temperate and the vegetation is characterised mostly by deciduous broad-leaved forests. The peak of fire activity tends to be just after snowmelt and before leaf production and is mostly driven by short-term dryness of surface soil layers rather than long-term drought. The potential predictability of fires is lower than in the Mediterranean.

Finally, the large forests of South America and Central Africa are characterised by large seasonal fires mostly initiated by agricultural burning. The peak of the fire season is in August and September and coincides with the end of the dry season. Given the vast availability of fuel in these regions, the good predictability of fire conditions can be

Useful links

GEO programme for a Global Wildfire Information System (GWIS):
https://www.earthobservations.org/activity.php?id=42

GWIS viewer:
http://forest.jrc.ec.europa.eu/effis/applications/global-viewer/

attributed to the good representation of dry conditions in the reanalysis dataset.

What next?

We have shown that fire danger modelling based on weather forecasts can provide reasonable potential predictability over large parts of the global landmass. However, in order to cover the disaster management cycle, the mere provision of model output is not enough. It is necessary to link early warning systems, such as EFFIS/GEFF, to response actions. This will require a closer link between the developer of the modelling components and the disaster management services to develop products tailored to supporting all phases of fire management. The ultimate aim is a more effective response to emergencies and cost reductions for society.

Systems such as EFFIS/GEFF can help by providing an efficient and cost-effective way to understand the behaviour of wildfires and to be able to forecast their occurrence and spread. This makes it possible to take appropriate action to fight fires with the required resources in strategic points. Most probably, these strategic points are not even burning yet. Being able to assess the danger and the overall situation is essential to making the right short- and long-term tactical and strategic decisions. This is true of all stakeholders, from civil protection agencies and first responders to operators of critical infrastructure, insurance companies and affected citizens.

The ability to provide such assessments well into the future is where the strength of the EFFIS/GEFF system lies. The system could prove particularly useful if mechanisms were established at the national and European level (e.g. involving the EU Civil Protection Mechanism/Emergency Response Coordination Centre (ERCC)) so that modelling results can be translated into decisions.

FURTHER READING

Di Giuseppe, **F.**, **F. Pappenberger**, **F. Wetterhall**, **B. Krzeminski**, **A. Camia**, **J. San-Miguel-Ayanz**, **G. Libertà**, 2016: The potential predictability of fire danger provided by numerical weather prediction. *J. Appl. Meteorol. and Climatol.* (under review)

ECMWF Calendar 2016

Apr 25	Policy Advisory Committee
Apr 25–26	ERA-CLIM2 Review and Progress Meeting
Apr 26–27	Finance Committee
May 8–12	Cray User Group Meeting (London)
May 9–13	NWP Training Course: Predictability and Ocean–Atmosphere Ensemble Forecasting
May 16–20	NWP Training Course: Parametrization of Subgrid Physical Processes
May 17–18	Security Representatives' Meeting
May 18–20	Computing Representatives' Meeting
May 31 – Jun 1	Technical Advisory Committee subgroup on verification measures
Jun 6–9	Using ECMWF's Forecasts (UEF)
Jun 30 – Jul 1	Council
Sep 5–8	Annual Seminar
Sep 12–16	Workshop on Drag Processes and Links to Large-Scale Circulation
Sep 26–30	Computer User Training Course: Data Analysis and Visualisation using Metview
Sep 29–30	Working Group for Co-operation between European Forecasters (WGCEF)
Oct 3–6	Workshop on Numerical and Computational Methods for Simulation of All-Scale Geophysical Flows
Oct 3–6	Training Course: Use and Interpretation of ECMWF Products
Oct 10–12	Scientific Advisory Committee
Oct 13-14	Technical Advisory Committee
Oct 17	Policy Advisory Committee
Oct 18–19	Finance Committee
Oct 18–21	Earth Radiation Budget Workshop
Oct 24–28	Workshop on High-Performance Computing in Meteorology
Nov 7–11	Workshop on Tropical Modelling and Assimilation
Nov 15–17	EUMETSAT Satellite Application Facility on Climate Monitoring (CM SAF) Workshop
Nov 21–25	UERRA General Assembly
Nov 29–30	ECOMET General Assembly and EUMETNET Assembly
Dec 1–2	Council

ECMWF publications

(see http://www.ecmwf.int/en/research/publications)

Technical Memoranda

775 **Janssen**, **P.A.E.M.**: How rare is the Draupner wave event? *December 2015*

774 **Trigo**, **I. F.**, **S. Boussetta**, **P. Viterbo**, **G. Balsamo**: Comparison of model land skin temperature with remotely sensed estimates and assessment of surface-atmosphere coupling. *December 2015*

773 **Agusti-Panareda**, **A.**, **S. Massart**, **F. Chevallier**, **G. Balsamo**, **S. Boussetta, E. Dutra**, **A. Beljaars**: A biogenic CO2 flux adjustment scheme for the mitigation of large-scale biases in global atmospheric CO2 analyses and forecasts. *December 2015*

772 **P. Lopez**: A lightning parameterization for the ECMWF model. *January 2016*

771 **Zagar**, **N.**, **R. Buizza**, **J. Tribbia**: A three-dimensional multivariate modal analysis of atmospheric predictability with application to the ECMWF ensemble. *November 2015*

769 **Rodwell**, **M.**, **L. Ferranti**, **L. Magnusson**: Diagnosis of northern hemispheric regime behaviour during winter 2013/14. *November 2015*

768 **Diamantakis**, **M.**, **L. Magnusson**: Numerical sensitivity of the ECMWF model to Semi-Lagrangian departure point iterations. *December 2015*

EUMETSAT/ECMWF Fellowship Programme Research Reports

40 **Letertre-Danczak**, **J.**: The use of geostationary radiance observations at ECMWF and aerosol detection for hyper-spectral infrared sounders: 1st and 2nd years report. *February 2016*

Contact information

ECMWF, Shinfield Park, Reading, Berkshire RG2 9AX, UK

Telephone National 0118 949 9000

Telephone International +44 118 949 9000

Fax +44 118 986 9450

ECMWF's public website http://www.ecmwf.int/

E-mail: The e-mail address of an individual at the Centre is firstinitial.lastname@ecmwf.int. For double-barrelled names use a hyphen (e.g. j-n.name-name@ecmwf.int).

Problems, queries and advice	Contact
General problems, fault reporting, web access and service queries	calldesk@ecmwf.int
Advice on the usage of computing and archiving services	advisory@ecmwf.int
Queries regarding access to data	data.services@ecmwf.int
Queries regarding the installation of ECMWF software packages	software.support@ecmwf.int
Queries or feedback regarding the forecast products	forecast_user@ecmwf.int

Index of newsletter articles

This is a selection of articles published in the *ECMWF Newsletter* series during recent years.
Articles are arranged in date order within each subject category.
Articles can be accessed on the ECMWF public website – http://www.ecmwf.int/en/research/publications

ECMWF
Newsletter | Number 147 – Spring 2016
European Centre for Medium-Range Weather Forecasts
www.ecmwf.int